Supporting Information

Studying 'Invisible' Excited Protein States in Slow Exchange with a Major State Conformation

Pramodh Vallurupalli[1,*] , Guillaume Bouvignies[1] and Lewis E. Kay[1,2,*]

[1]Departments of Molecular Genetics, Biochemistry and Chemistry, The University of Toronto, Toronto, Ontario, M5S 1A8, Canada

[2]Hospital for Sick Children, Program in Molecular Structure and Function, 555 University Avenue, Toronto, Ontario, M5G 1X8, Canada

Table 1A. Values of $\Delta\varpi$, R_2^G, R_2^E, R_1^G obtained from fits of CEST profiles recorded on the Abp1p-Ark1p system, 1ºC, 11.7T to a global two-site exchange processes. The six residues that showed clear evidence for a second state (well resolved dips for both ground and excited states in profiles) were used in the fit. Optimal values of (k_{ex},p_E)=(130±4 s^{-1},2.38±0.04%) were obtained.

Residue	$\Delta\varpi$ (ppm)	R_2^G (s^{-1})	R_2^E (s^{-1})	R_1^G (s^{-1})
15	-1.98 ± 0.02	8.27 ± 0.13	13.4 ± 4.6	1.67 ± 0.01
31	2.06 ± 0.02	9.73 ± 0.14	6.4 ± 4.8	1.64 ± 0.01
32	-8.82 ± 0.01	7.71 ± 0.14	19.9 ± 5.9	1.70 ± 0.01
33	2.27 ± 0.02	8.11 ± 0.15	13.2 ± 5.7	1.97 ± 0.01
34	4.52 ± 0.01	8.07 ± 0.14	27.1 ± 5.3	1.70 ± 0.01
37	-1.94 ± 0.03	9.79 ± 0.26	0.0 ± 4.9	1.96 ± 0.01

Table 1B. Values of $\Delta\varpi$, R_2^G, R_2^E, R_1^G obtained from fits of all CEST profiles recorded on the Abp1p-Ark1p system, 1°C, 11.7T to a global two-site exchange processes. Values of (k_{ex},p_E) were fixed to (130 s^{-1}, 2.38%) and profiles for all of the residues fit simultaneously.

Residue	$\Delta\varpi$ (ppm)	R_2^G (s^{-1})	R_2^E (s^{-1})	R_1^G (s^{-1})
1	-0.16 ± 0.07	5.33 ± 0.25	0.7 ± 10.2	1.60 ± 0.01
3	0.26 ± 0.05	8.71 ± 0.36	4.8 ± 14.5	1.87 ± 0.01
4	0.37 ± 0.06	8.78 ± 0.39	2.6 ± 15.5	2.02 ± 0.01
5	0.47 ± 0.04	9.63 ± 0.30	16.4 ± 11.8	1.88 ± 0.01
6	0.11 ± 0.06	7.09 ± 0.45	94.7 ± 28.5	1.97 ± 0.01
7	-0.11 ± 0.21	9.28 ± 1.39	12.3 ± 60.4	1.98 ± 0.02
8	-0.76 ± 0.03	8.87 ± 0.25	5.7 ± 8.5	1.92 ± 0.01
9	0.36 ± 0.03	8.48 ± 0.23	0.1 ± 8.8	1.66 ± 0.01
10	0.57 ± 0.04	9.57 ± 0.24	19.4 ± 9.5	1.96 ± 0.01
11	-0.41 ± 0.03	8.52 ± 0.21	3.8 ± 8.7	1.75 ± 0.01
12	0.28 ± 0.06	8.46 ± 0.32	2.4 ± 13.4	1.81 ± 0.01
13	-0.49 ± 0.03	8.72 ± 0.25	10.9 ± 9.8	1.81 ± 0.01
14	-0.53 ± 0.03	8.05 ± 0.22	3.2 ± 8.1	1.64 ± 0.01
15	-1.98 ± 0.01	8.27 ± 0.10	13.4 ± 3.6	1.67 ± 0.01
16	-0.64 ± 0.02	8.18 ± 0.19	18.6 ± 7.7	1.79 ± 0.01
17	-1.07 ± 0.02	9.64 ± 0.14	7.1 ± 4.5	1.86 ± 0.01
18	-0.57 ± 0.05	9.49 ± 0.34	1.3 ± 12.2	2.05 ± 0.01
19	-0.39 ± 0.03	8.16 ± 0.19	4.8 ± 7.6	1.67 ± 0.01
20	0.21 ± 0.09	9.19 ± 0.65	17.1 ± 28.3	1.98 ± 0.01
21	-0.16 ± 0.09	9.45 ± 0.60	2.9 ± 24.9	1.86 ± 0.01
22	0.25 ± 0.06	7.92 ± 0.39	58.4 ± 21.5	1.78 ± 0.01
23	-0.26 ± 0.06	8.36 ± 0.35	15.2 ± 15.7	1.91 ± 0.01
24	0.27 ± 0.07	9.65 ± 0.38	7.4 ± 16.3	1.89 ± 0.01
25	0.25 ± 0.06	8.53 ± 0.37	2.6 ± 14.8	1.77 ± 0.01
27	-0.20 ± 0.09	8.39 ± 0.77	39.7 ± 38.3	1.99 ± 0.01
28	-0.14 ± 0.07	8.46 ± 0.56	47.8 ± 28.9	1.81 ± 0.01
29	-0.06 ± 0.23	9.12 ± 2.46	22.7 ± 110	1.98 ± 0.03
30	-0.54 ± 0.03	9.35 ± 0.23	3.0 ± 7.7	1.87 ± 0.01
31	2.06 ± 0.02	9.73 ± 0.13	6.3 ± 4.2	1.64 ± 0.01
32	-8.82 ± 0.01	7.71 ± 0.13	19.9 ± 5.2	1.70 ± 0.01
33	2.27 ± 0.02	8.12 ± 0.18	13.1 ± 6.9	1.97 ± 0.01
34	4.52 ± 0.01	8.07 ± 0.11	27.7 ± 4.4	1.70 ± 0.01
35	-1.02 ± 0.02	8.36 ± 0.16	22.2 ± 6.0	1.84 ± 0.01
36	-1.13 ± 0.03	8.47 ± 0.23	12.8 ± 8.0	1.83 ± 0.01
37	-1.95 ± 0.04	9.91 ± 0.28	4.0 ± 8.8	1.96 ± 0.01
38	-0.30 ± 0.07	9.29 ± 0.51	2.5 ± 19.4	1.90 ± 0.01
39	0.47 ± 0.05	9.60 ± 0.34	18.1 ± 13.8	1.93 ± 0.01
40	0.30 ± 0.03	2.94 ± 0.14	0.8 ± 5.5	1.48 ± 0.01
41	0.33 ± 0.06	9.51 ± 0.33	2.4 ± 13.3	2.00 ± 0.01
42	-0.35 ± 0.04	8.55 ± 0.25	0.2 ± 10.1	1.96 ± 0.01
43	-0.17 ± 0.13	8.43 ± 0.71	18.4 ± 33.0	1.89 ± 0.01
44	-0.37 ± 0.04	8.49 ± 0.29	1.5 ± 11.2	1.96 ± 0.01
45	-0.21 ± 0.08	8.98 ± 0.46	0.6 ± 18.4	1.92 ± 0.01
46	-0.29 ± 0.06	8.36 ± 0.44	25.1 ± 20.2	1.91 ± 0.01
47	-0.05 ± 0.04	7.20 ± 0.37	66.9 ± 20.6	1.70 ± 0.01
48	0.20 ± 0.10	8.93 ± 0.68	23.8 ± 31.6	1.91 ± 0.01
49	-0.83 ± 0.03	9.55 ± 0.22	15.9 ± 8.5	1.84 ± 0.01
50	0.19 ± 0.12	9.78 ± 0.69	1.2 ± 27.9	2.04 ± 0.01
52	-1.14 ± 0.03	12.14 ± 0.23	44.7 ± 9.1	1.88 ± 0.01
53	0.87 ± 0.04	12.74 ± 0.33	0.4 ± 10.1	1.85 ± 0.01

54	0.24 ± 0.09	9.45 ± 0.64	5.9 ± 26.8	1.99 ± 0.01
55	−0.52 ± 0.06	9.97 ± 0.32	176.8 ± 26.0	1.95 ± 0.01
56	0.33 ± 0.06	9.46 ± 0.42	35.4 ± 20.0	1.87 ± 0.01
57	−0.28 ± 0.06	9.26 ± 0.38	39.7 ± 19.0	1.76 ± 0.01
58	−0.25 ± 0.07	8.89 ± 0.46	2.2 ± 18.0	1.91 ± 0.01
59	−0.29 ± 0.06	6.60 ± 0.37	0.5 ± 14.9	1.71 ± 0.01

Supporting Figure 1. Intensity profiles (red) and best fits (blue) from the global fit of the six residues in the Abp1p-Ark1p exchanging system, 1^{o}C, 11.7T, showing clear evidence of a second state.

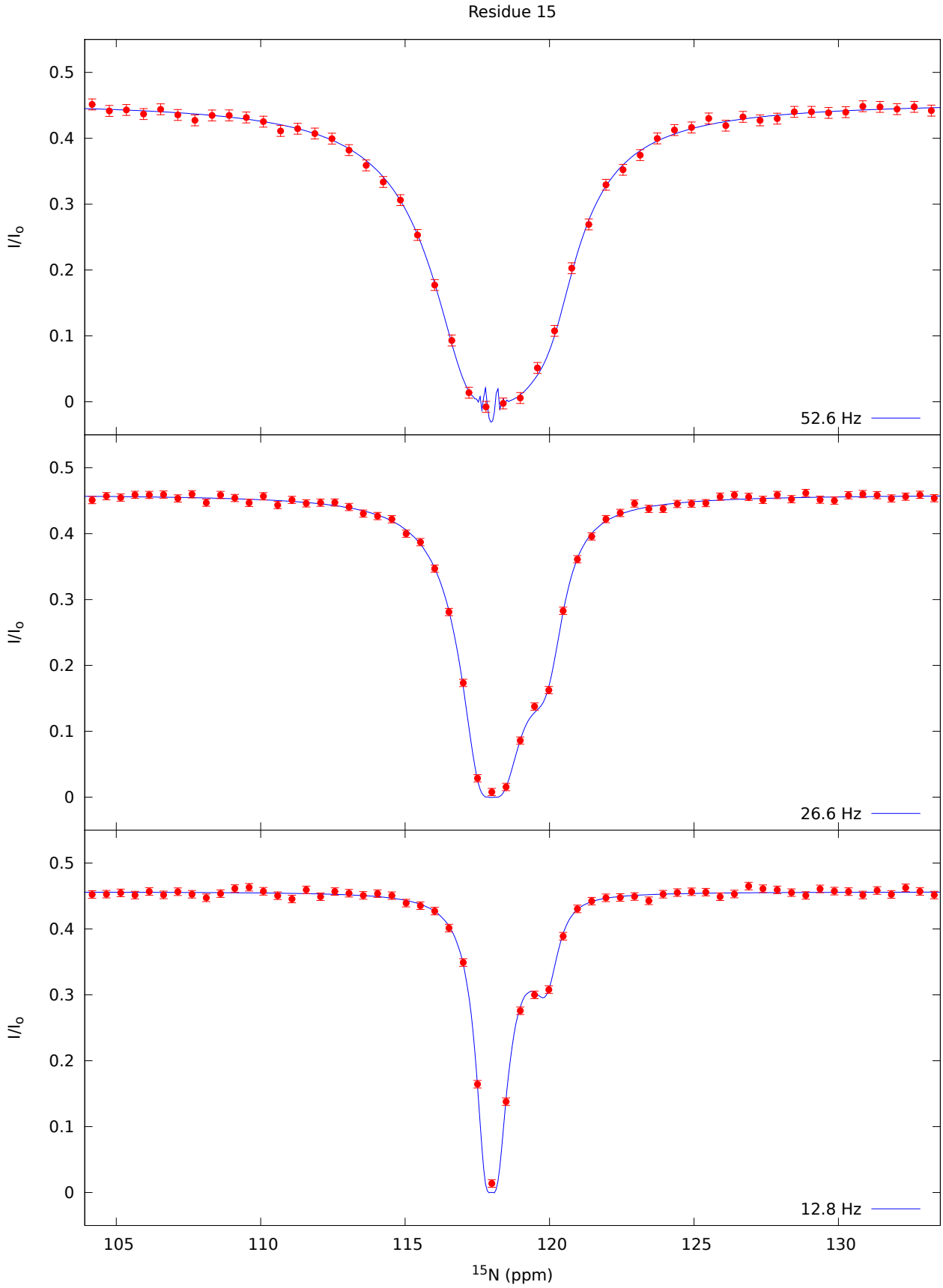
Residue 15
I/I$_o$
0.5
0.4
0.3
0.2
0.1
0
52.6 Hz
26.6 Hz
12.8 Hz
105
110
115
120
125
130
^{15}N (ppm)

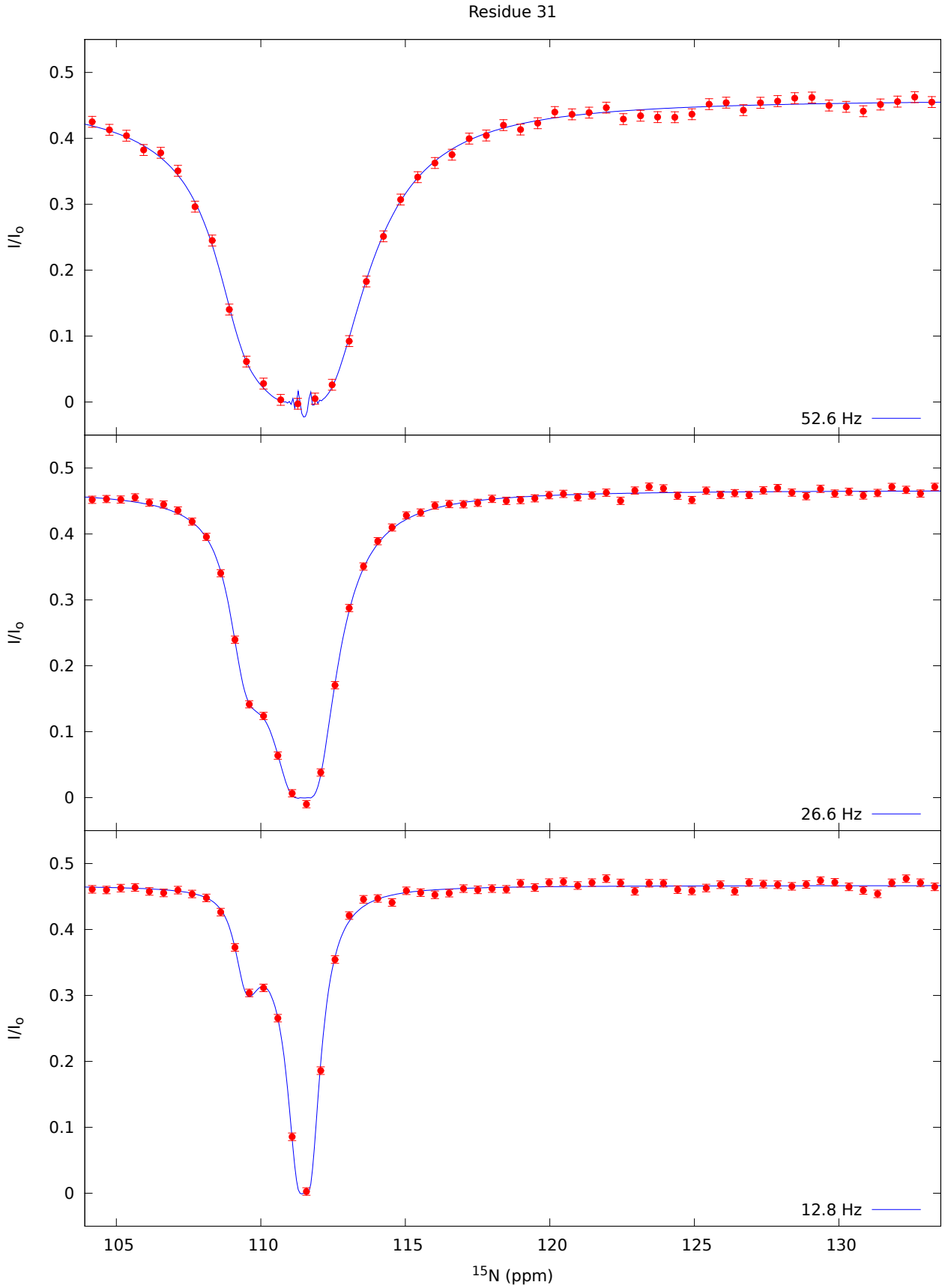
Residue 31
I/I$_o$
0.5
0.4
0.3
0.2
0.1
0
52.6 Hz
26.6 Hz
12.8 Hz
105
110
115
120
125
130
^{15}N (ppm)

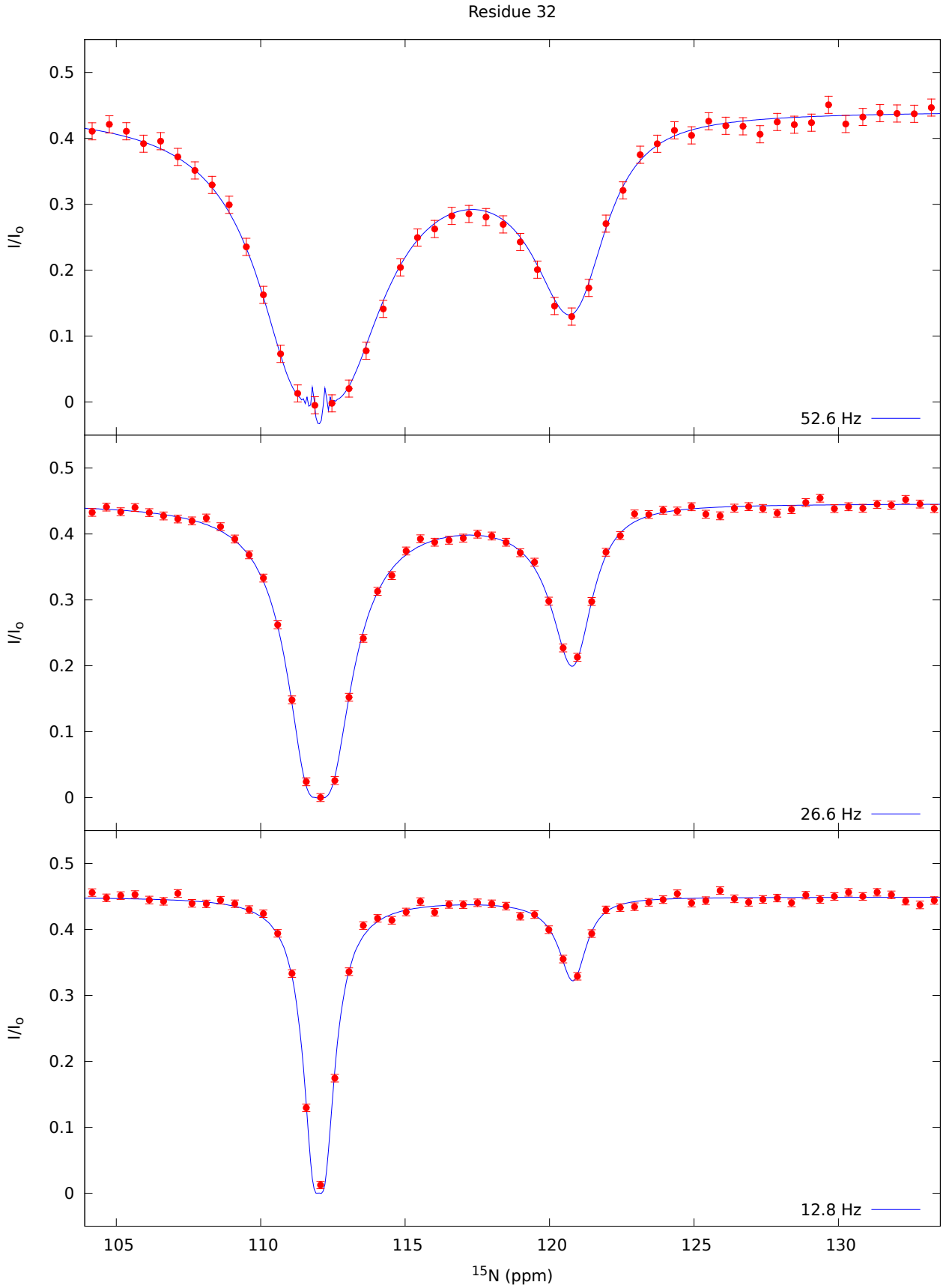
Residue 32
I/I$_o$
52.6 Hz
26.6 Hz
12.8 Hz
^{15}N (ppm)

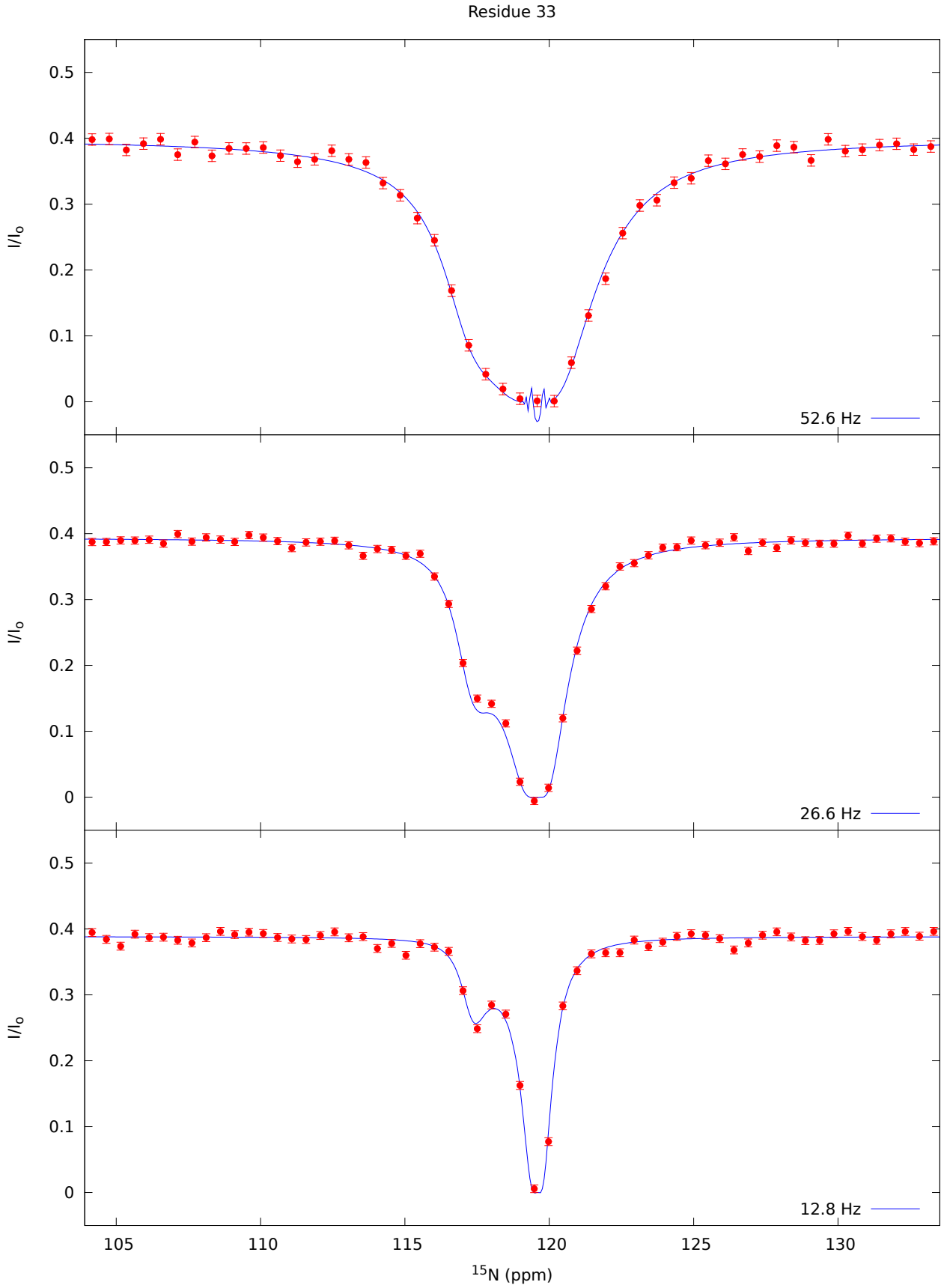
Residue 33
I/I$_o$
52.6 Hz
26.6 Hz
12.8 Hz
^{15}N (ppm)

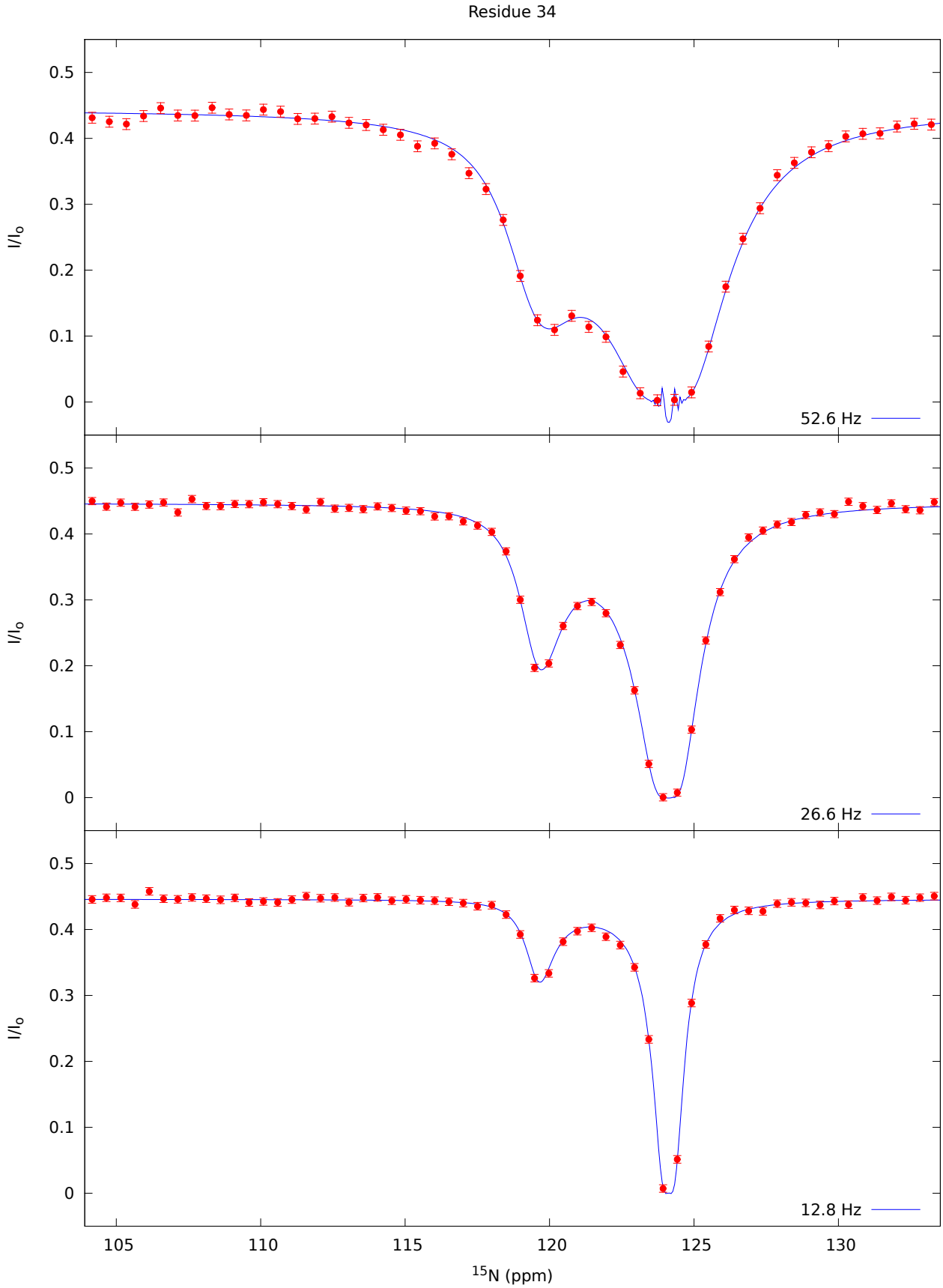
Residue 34
I/I$_o$
0.5
0.4
0.3
0.2
0.1
0
52.6 Hz
26.6 Hz
12.8 Hz
105
110
115
120
125
130
^{15}N (ppm)

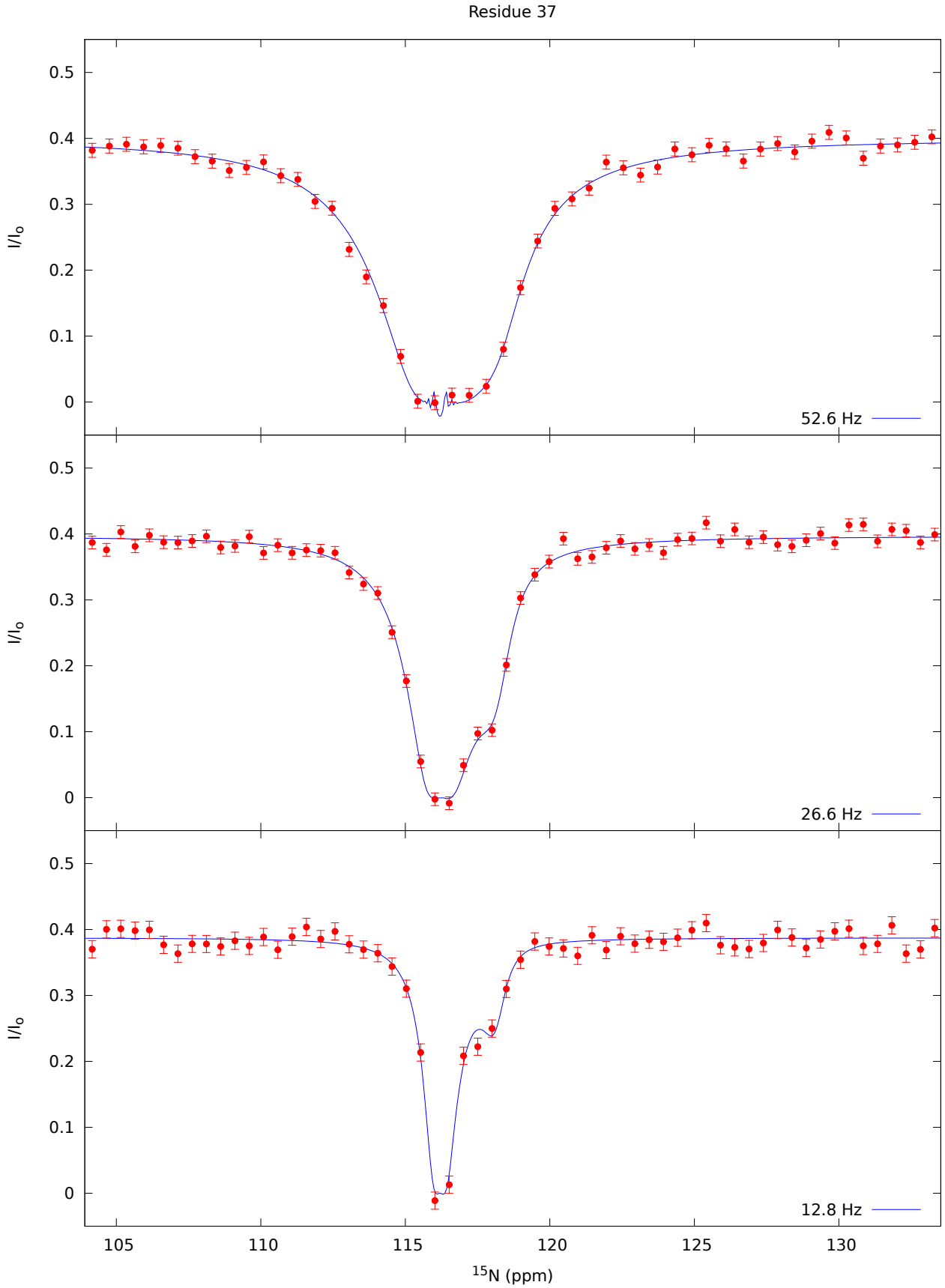
Residue 37
I/I$_o$
0.5
0.4
0.3
0.2
0.1
0
52.6 Hz
26.6 Hz
12.8 Hz
105
110
115
120
125
130
^{15}N (ppm)

Table 2A. Values of $\Delta\varpi$, R_2^G, R_2^E, R_1^G obtained from fits of CEST profiles recorded on the A39G FF domain 1ºC, 11.7T to a global two-site exchange processes. The 37 residues that showed clear evidence for a second state (well resolved dips for both ground and excited states in profiles) were used in the fit. Optimal values of (k_{ex}, p_E)=(51.6±0.7 s^{-1},1.65±0.014%) were obtained.

Residue	$\Delta\varpi$ (ppm)	R_2^G (s^{-1})	R_2^E (s^{-1})	R_1^G (s^{-1})
10	1.68 ± 0.02	10.36 ± 0.11	26.6 ± 5.0	1.45 ± 0.01
13	4.23 ± 0.02	14.01 ± 0.09	119.4 ± 6.8	1.22 ± 0.01
15	1.89 ± 0.02	12.00 ± 0.08	35.2 ± 3.9	1.39 ± 0.01
18	2.15 ± 0.01	12.36 ± 0.08	38.7 ± 4.0	1.40 ± 0.01
22	3.34 ± 0.02	12.47 ± 0.08	74.7 ± 5.3	1.42 ± 0.01
25	2.76 ± 0.02	12.88 ± 0.09	62.2 ± 5.2	1.46 ± 0.01
26	5.25 ± 0.02	12.58 ± 0.08	92.1 ± 5.6	1.42 ± 0.01
27	-1.94 ± 0.02	12.77 ± 0.10	64.1 ± 6.3	1.43 ± 0.01
28	6.70 ± 0.02	11.95 ± 0.08	203.8 ± 9.5	1.44 ± 0.01
29	5.85 ± 0.02	12.27 ± 0.09	162.2 ± 9.4	1.41 ± 0.01
33	4.28 ± 0.02	11.89 ± 0.08	85.2 ± 5.6	1.48 ± 0.01
37	4.78 ± 0.02	12.89 ± 0.09	100.1 ± 6.7	1.38 ± 0.01
38	2.43 ± 0.01	13.06 ± 0.10	18.3 ± 5.0	1.41 ± 0.01
39	1.49 ± 0.01	12.77 ± 0.09	29.2 ± 4.3	1.43 ± 0.01
41	6.15 ± 0.02	14.00 ± 0.08	102.8 ± 5.9	1.36 ± 0.01
42	6.23 ± 0.02	12.74 ± 0.10	164.0 ± 9.9	1.41 ± 0.01
43	12.46 ± 0.03	12.76 ± 0.10	216.5 ± 12.0	1.41 ± 0.01
44	3.45 ± 0.03	13.62 ± 0.11	196.2 ± 12.1	1.38 ± 0.01
45	3.80 ± 0.02	13.21 ± 0.08	161.0 ± 8.4	1.36 ± 0.01
48	2.27 ± 0.01	12.11 ± 0.09	28.6 ± 3.6	1.46 ± 0.01
50	8.20 ± 0.01	12.22 ± 0.08	69.7 ± 4.5	1.43 ± 0.01
51	1.54 ± 0.02	13.12 ± 0.10	58.1 ± 6.4	1.48 ± 0.01
52	8.42 ± 0.01	14.23 ± 0.15	21.9 ± 6.1	1.41 ± 0.01
53	-2.80 ± 0.01	10.87 ± 0.07	47.1 ± 4.4	1.33 ± 0.01
54	3.25 ± 0.01	10.55 ± 0.07	69.0 ± 4.7	1.32 ± 0.01
55	-6.38 ± 0.02	11.88 ± 0.10	34.8 ± 4.3	1.45 ± 0.01
56	3.64 ± 0.02	12.17 ± 0.09	87.5 ± 6.3	1.41 ± 0.01
59	6.30 ± 0.01	12.81 ± 0.10	38.4 ± 5.3	1.43 ± 0.01
60	2.40 ± 0.01	12.68 ± 0.09	33.4 ± 4.5	1.38 ± 0.01
61	2.22 ± 0.01	12.96 ± 0.09	18.2 ± 3.5	1.44 ± 0.01
63	2.93 ± 0.01	12.37 ± 0.09	39.4 ± 4.6	1.43 ± 0.01
64	2.08 ± 0.01	12.54 ± 0.09	20.2 ± 3.3	1.41 ± 0.01
65	-1.64 ± 0.01	11.93 ± 0.09	20.8 ± 4.5	1.43 ± 0.01
66	4.18 ± 0.01	12.29 ± 0.08	48.9 ± 4.7	1.45 ± 0.01
67	8.04 ± 0.01	12.20 ± 0.08	61.9 ± 4.2	1.39 ± 0.01
68	4.38 ± 0.01	10.57 ± 0.07	43.6 ± 3.9	1.46 ± 0.01
69	1.85 ± 0.01	7.75 ± 0.07	11.7 ± 3.6	1.56 ± 0.01

Table 2B. Values of $\Delta\varpi$, R_2^G, R_2^E, R_1^G obtained from fits of all CEST profiles recorded on the A39G FF domain, 1ºC, 11.7T to a global two-site exchange processes. Values of (k_{ex},p_E) were fixed to (51.6 s^{-1},1.65%) and profiles for all of the residues fit simultaneously.

Residue	$\Delta\varpi$ (ppm)	R_2^G (s^{-1})	R_2^E (s^{-1})	R_1^G (s^{-1})
3	0.18 ± 0.03	1.81 ± 0.09	0.9 ± 5.2	1.19 ± 0.01
5	-0.13 ± 0.03	2.74 ± 0.08	0.3 ± 4.3	1.43 ± 0.01
6	-0.22 ± 0.01	3.57 ± 0.07	0.0 ± 3.3	1.49 ± 0.01
7	-0.13 ± 0.02	5.07 ± 0.06	0.5 ± 3.7	1.56 ± 0.01
8	-0.96 ± 0.01	8.33 ± 0.07	7.9 ± 2.9	1.54 ± 0.01
9	-0.22 ± 0.03	7.58 ± 0.11	19.1 ± 7.1	1.53 ± 0.01
10	1.68 ± 0.02	10.32 ± 0.11	27.2 ± 5.2	1.45 ± 0.01
11	1.36 ± 0.05	16.17 ± 0.33	42.5 ± 18.4	1.41 ± 0.01
12	0.45 ± 0.02	13.96 ± 0.14	1.0 ± 7.0	1.37 ± 0.01
13	4.23 ± 0.02	13.96 ± 0.08	120.2 ± 6.3	1.23 ± 0.01
14	-0.32 ± 0.03	11.67 ± 0.15	14.6 ± 8.8	1.45 ± 0.01
15	1.89 ± 0.01	11.95 ± 0.07	35.7 ± 3.4	1.39 ± 0.01
16	1.30 ± 0.01	11.16 ± 0.09	26.0 ± 4.8	1.44 ± 0.01
17	-1.11 ± 0.02	12.92 ± 0.11	13.1 ± 3.9	1.47 ± 0.01
18	2.15 ± 0.01	12.31 ± 0.09	39.3 ± 4.3	1.40 ± 0.01
19	0.92 ± 0.02	12.62 ± 0.08	39.1 ± 4.6	1.41 ± 0.01
20	-0.18 ± 0.07	12.79 ± 0.40	66.5 ± 33.9	1.48 ± 0.01
21	0.41 ± 0.03	11.45 ± 0.12	33.4 ± 7.8	1.52 ± 0.01
22	3.34 ± 0.02	12.42 ± 0.08	75.1 ± 5.4	1.42 ± 0.01
23	-0.17 ± 0.04	12.77 ± 0.25	33.9 ± 18.1	1.44 ± 0.01
24	-0.36 ± 0.03	12.27 ± 0.17	28.6 ± 10.9	1.47 ± 0.01
25	2.76 ± 0.02	12.83 ± 0.11	62.7 ± 6.4	1.46 ± 0.01
26	5.25 ± 0.02	12.54 ± 0.08	92.9 ± 5.9	1.42 ± 0.01
27	-1.94 ± 0.02	12.72 ± 0.09	64.8 ± 5.9	1.43 ± 0.01
28	6.70 ± 0.03	11.91 ± 0.09	204.9 ± 11.4	1.44 ± 0.01
29	5.85 ± 0.02	12.24 ± 0.09	163.1 ± 9.3	1.41 ± 0.01
30	1.52 ± 0.02	12.66 ± 0.08	88.2 ± 6.8	1.42 ± 0.01
32	0.35 ± 0.02	11.04 ± 0.10	28.4 ± 6.2	1.38 ± 0.01
33	4.28 ± 0.01	11.85 ± 0.07	85.8 ± 4.8	1.48 ± 0.01
34	0.77 ± 0.01	12.24 ± 0.07	17.8 ± 2.8	1.39 ± 0.01
35	-1.29 ± 0.01	11.26 ± 0.07	28.4 ± 3.9	1.46 ± 0.01
36	0.28 ± 0.03	12.74 ± 0.18	7.1 ± 8.4	1.43 ± 0.01
37	4.78 ± 0.02	12.85 ± 0.09	100.7 ± 6.3	1.38 ± 0.01
38	2.43 ± 0.01	13.01 ± 0.09	18.9 ± 4.5	1.41 ± 0.01
39	1.49 ± 0.01	12.71 ± 0.10	30.1 ± 4.5	1.43 ± 0.01
40	-0.97 ± 0.02	14.08 ± 0.09	14.6 ± 4.7	1.42 ± 0.01
41	6.15 ± 0.02	13.95 ± 0.09	103.4 ± 6.5	1.36 ± 0.01
42	6.23 ± 0.03	12.69 ± 0.11	165.0 ± 11.1	1.41 ± 0.01
43	12.46 ± 0.03	12.71 ± 0.12	217.1 ± 14.6	1.41 ± 0.01
44	3.44 ± 0.04	13.57 ± 0.12	197.0 ± 13.6	1.38 ± 0.01
45	3.80 ± 0.02	13.16 ± 0.07	161.9 ± 7.4	1.36 ± 0.01
46	0.42 ± 0.02	10.92 ± 0.07	28.2 ± 4.7	1.17 ± 0.01
48	2.27 ± 0.02	12.06 ± 0.10	29.0 ± 4.2	1.46 ± 0.01
50	8.20 ± 0.01	12.18 ± 0.08	70.1 ± 4.7	1.44 ± 0.01
51	1.53 ± 0.02	13.06 ± 0.09	59.5 ± 6.4	1.48 ± 0.01
52	8.42 ± 0.02	14.19 ± 0.21	21.9 ± 8.6	1.41 ± 0.01
53	-2.80 ± 0.01	10.83 ± 0.07	47.6 ± 4.4	1.33 ± 0.01
54	3.25 ± 0.01	10.51 ± 0.06	69.5 ± 3.8	1.32 ± 0.01

55	−6.38 ± 0.02	11.84 ± 0.10	35.0 ± 4.4	1.45 ± 0.01
56	3.64 ± 0.02	12.13 ± 0.09	88.1 ± 6.3	1.41 ± 0.01
57	0.56 ± 0.02	12.68 ± 0.11	38.2 ± 7.2	1.39 ± 0.01
58	0.87 ± 0.03	12.30 ± 0.14	40.3 ± 8.8	1.47 ± 0.01
59	6.30 ± 0.01	12.77 ± 0.12	38.5 ± 5.9	1.43 ± 0.01
60	2.40 ± 0.01	12.64 ± 0.06	33.9 ± 3.2	1.38 ± 0.01
61	2.22 ± 0.01	12.91 ± 0.08	18.8 ± 3.4	1.44 ± 0.01
62	−1.02 ± 0.01	12.39 ± 0.11	13.7 ± 4.5	1.47 ± 0.01
63	2.93 ± 0.01	12.33 ± 0.07	39.9 ± 4.0	1.43 ± 0.01
64	2.08 ± 0.01	12.49 ± 0.08	20.7 ± 3.4	1.41 ± 0.01
65	−1.64 ± 0.01	11.88 ± 0.09	21.7 ± 4.3	1.43 ± 0.01
66	4.18 ± 0.01	12.24 ± 0.09	49.5 ± 5.2	1.45 ± 0.01
67	8.04 ± 0.01	12.16 ± 0.07	62.0 ± 3.8	1.39 ± 0.01
68	4.38 ± 0.01	10.53 ± 0.05	44.0 ± 2.9	1.46 ± 0.01
69	1.85 ± 0.01	7.70 ± 0.04	12.5 ± 2.0	1.56 ± 0.01
70	0.57 ± 0.01	6.73 ± 0.03	3.1 ± 1.6	1.54 ± 0.01
71	−0.18 ± 0.01	4.34 ± 0.09	1.0 ± 5.0	1.50 ± 0.01

Supporting Figure 2. Intensity profiles (red) and best fits (blue) from the global fit of 37 residues of the A39G FF domain, 1^{o}C, 11.7T, showing clear evidence of exchange.

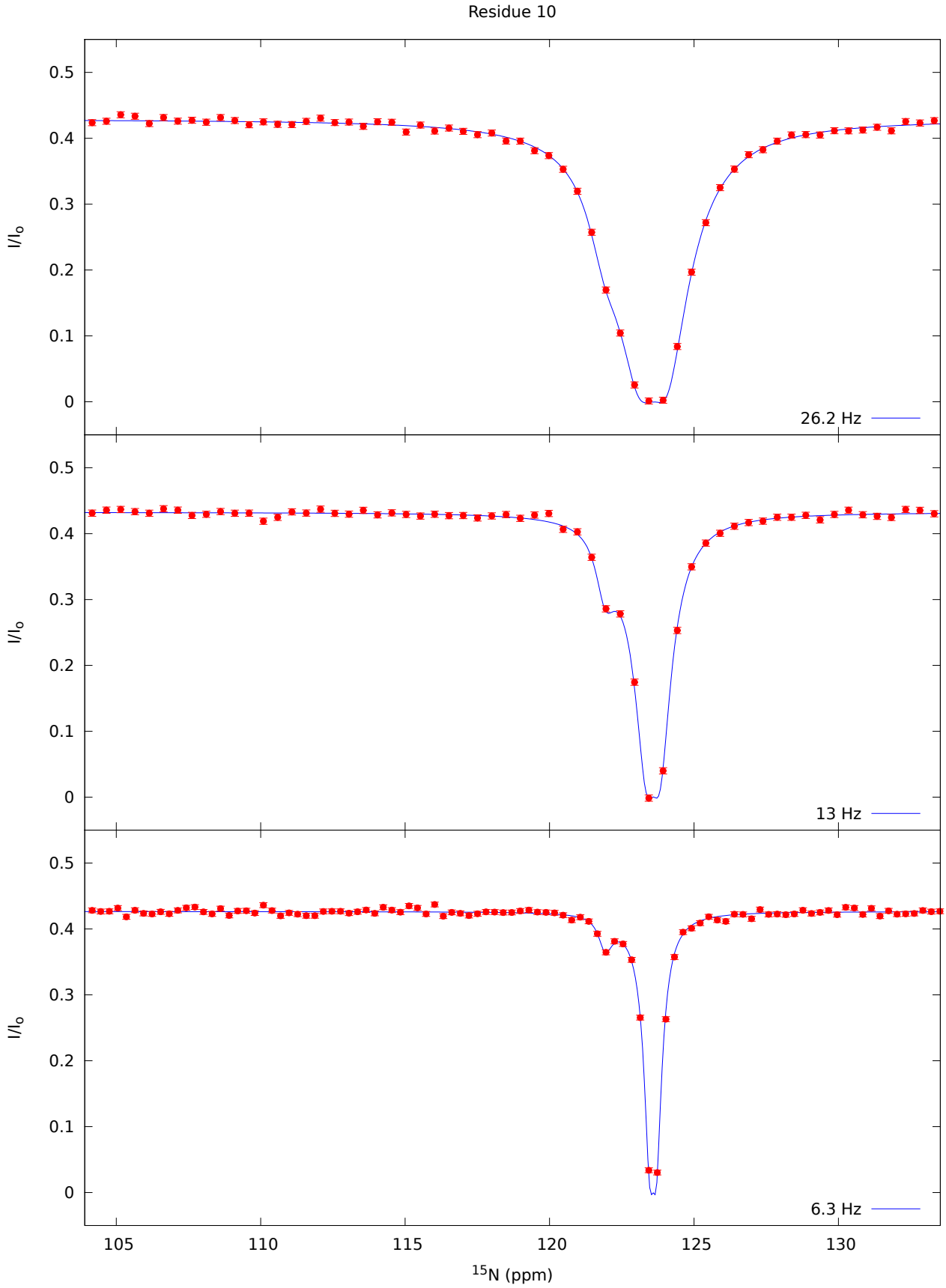
Residue 10
I/I$_o$
0.5
0.4
0.3
0.2
0.1
0
26.2 Hz
13 Hz
6.3 Hz
105
110
115
120
125
130
^{15}N (ppm)

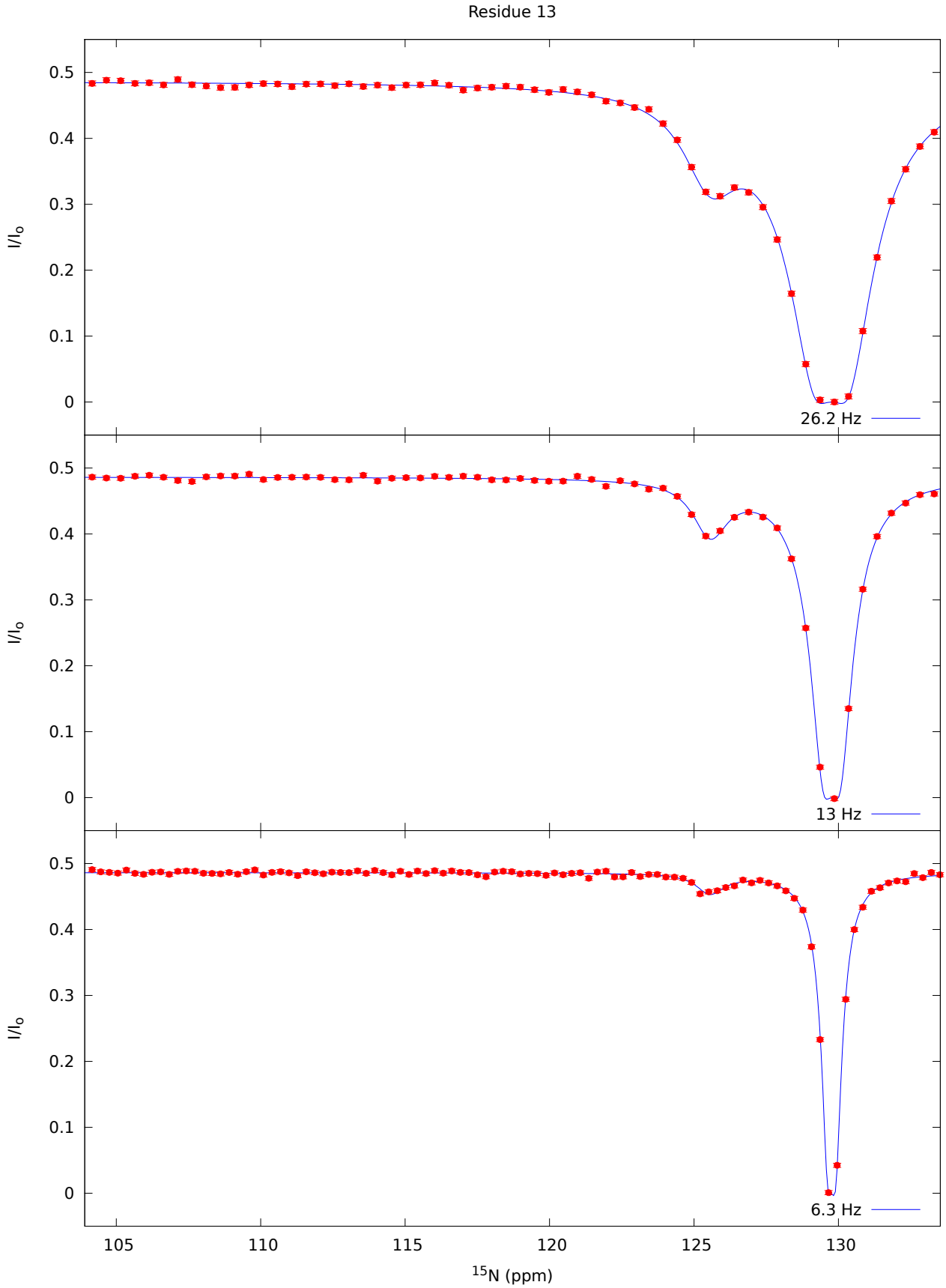
Residue 13
I/I$_o$
0.5
0.4
0.3
0.2
0.1
0
26.2 Hz
13 Hz
6.3 Hz
105
110
115
120
125
130
^{15}N (ppm)

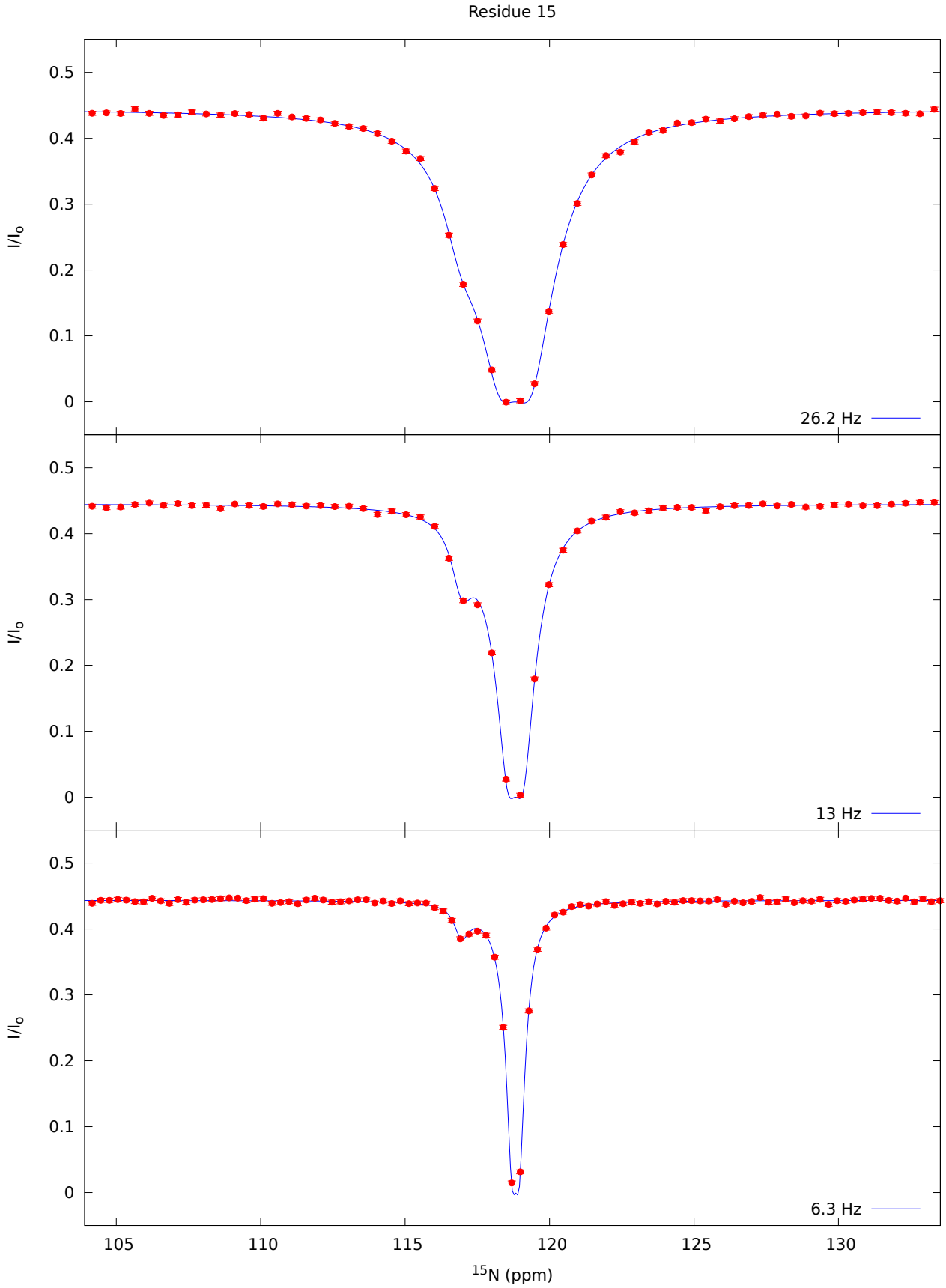
Residue 15
I/I$_o$
0.5
0.4
0.3
0.2
0.1
0
26.2 Hz
13 Hz
6.3 Hz
105
110
115
120
125
130
^{15}N (ppm)

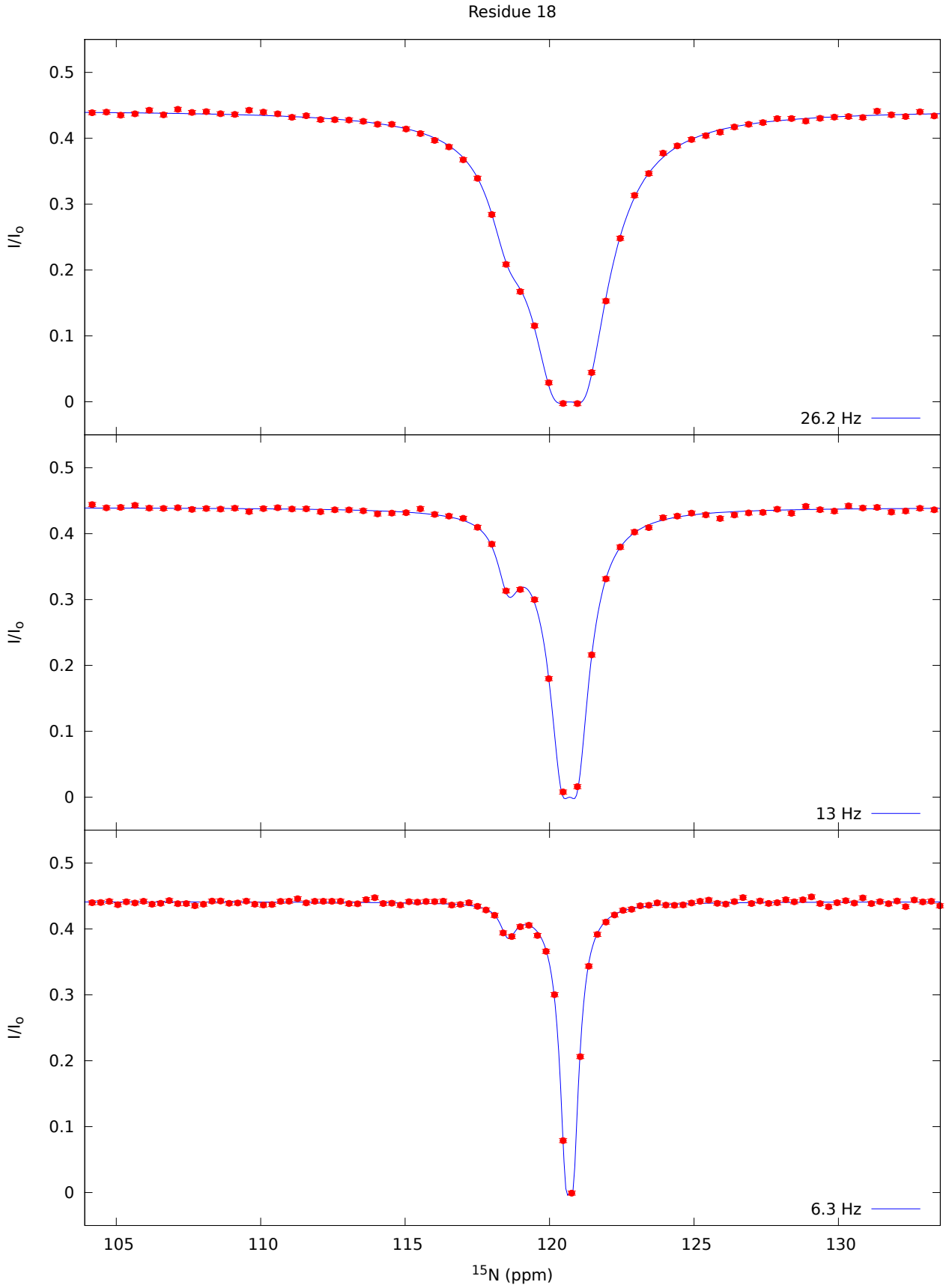
Residue 18
I/I$_o$
26.2 Hz
13 Hz
6.3 Hz
^{15}N (ppm)

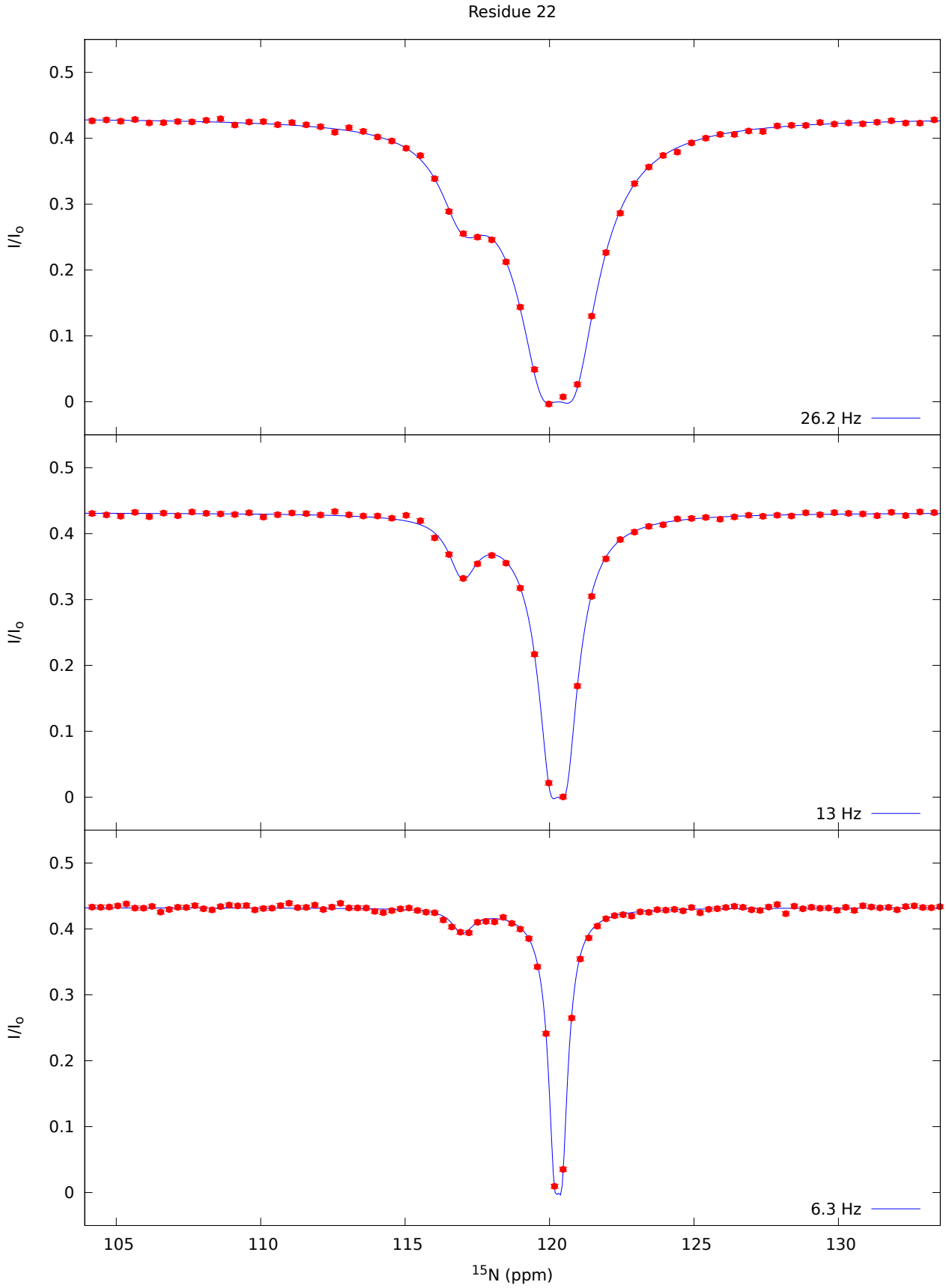
Residue 22
I/I$_o$
0.5
0.4
0.3
0.2
0.1
0
26.2 Hz
13 Hz
6.3 Hz
105
110
115
120
125
130
^{15}N (ppm)

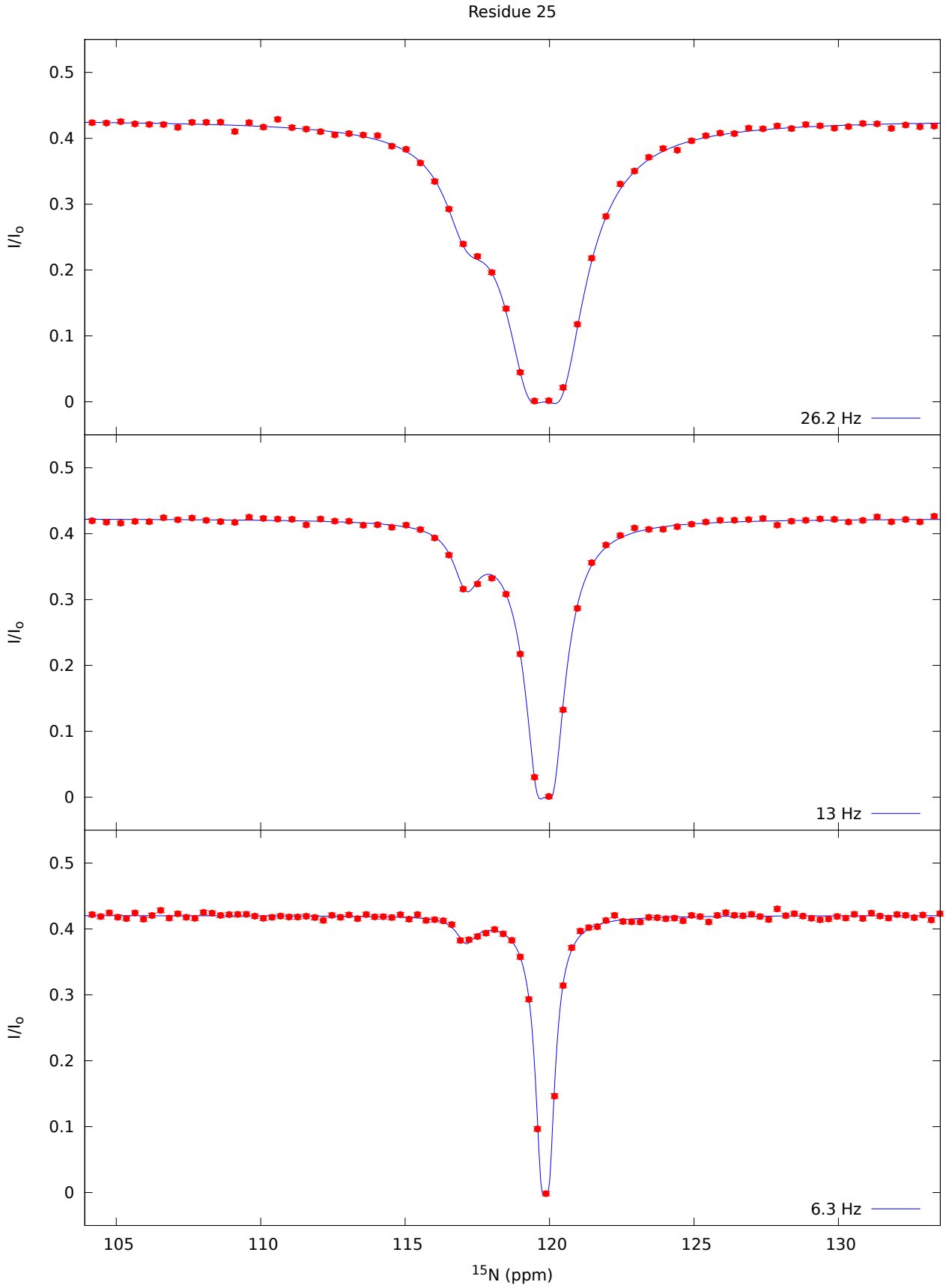
Residue 25
I/I$_o$
0.5
0.4
0.3
0.2
0.1
0
26.2 Hz
13 Hz
6.3 Hz
105
110
115
120
125
130
^{15}N (ppm)

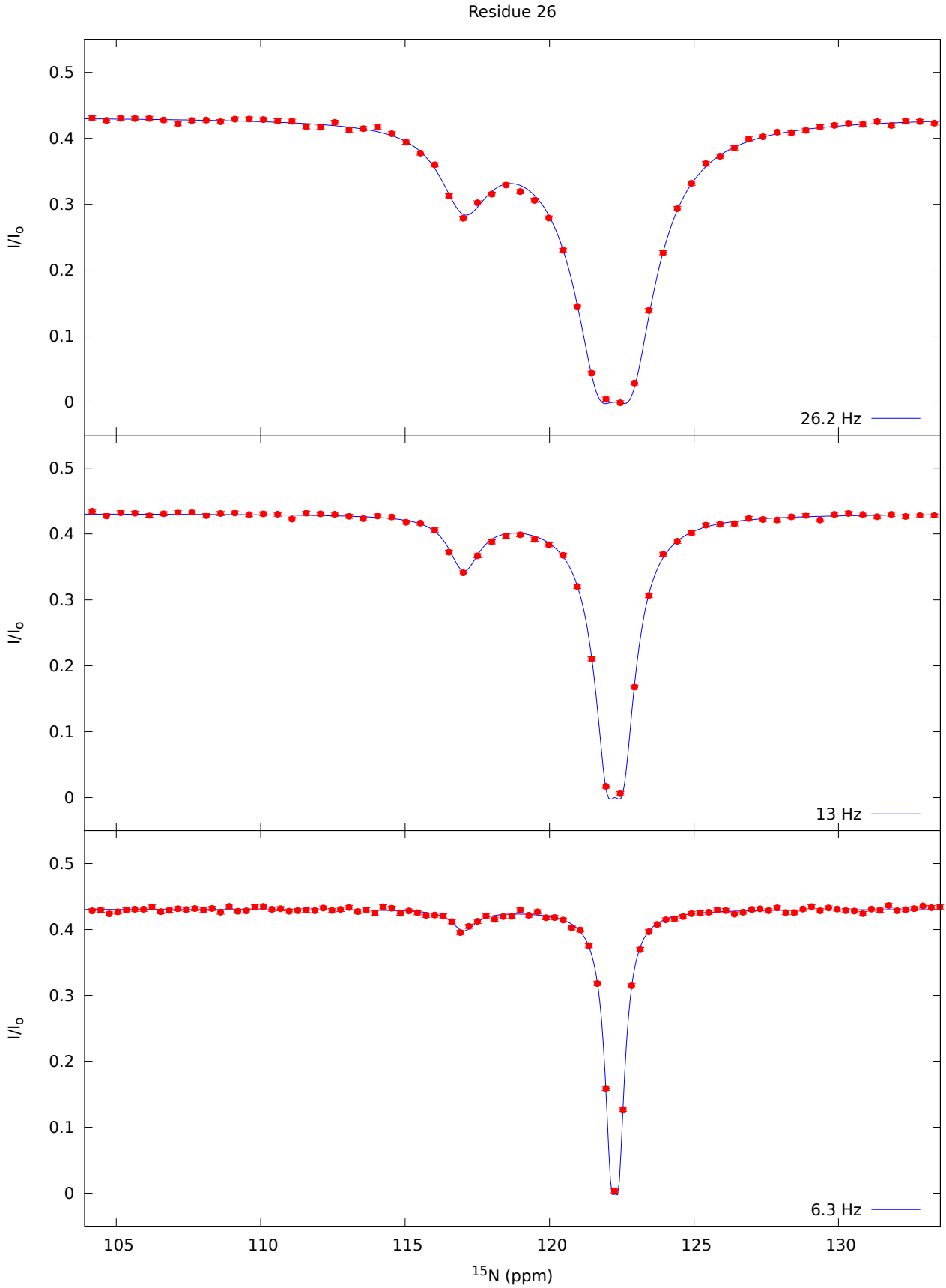
Residue 26
I/I$_o$
0.5
0.4
0.3
0.2
0.1
0
26.2 Hz
13 Hz
6.3 Hz
105
110
115
120
125
130
^{15}N (ppm)

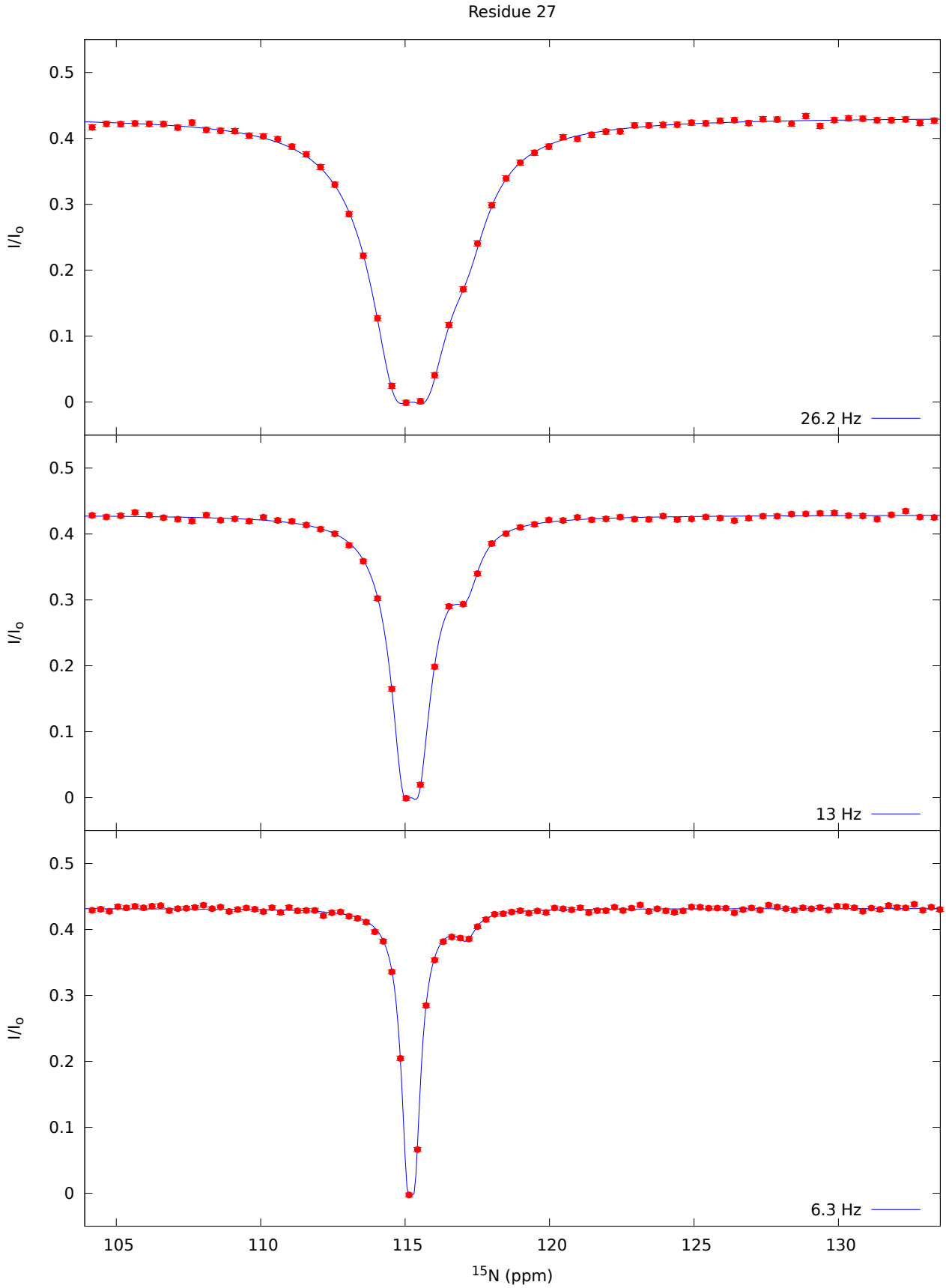
Residue 27
I/I$_o$
0.5
0.4
0.3
0.2
0.1
0
26.2 Hz
13 Hz
6.3 Hz
105
110
115
120
125
130
^{15}N (ppm)

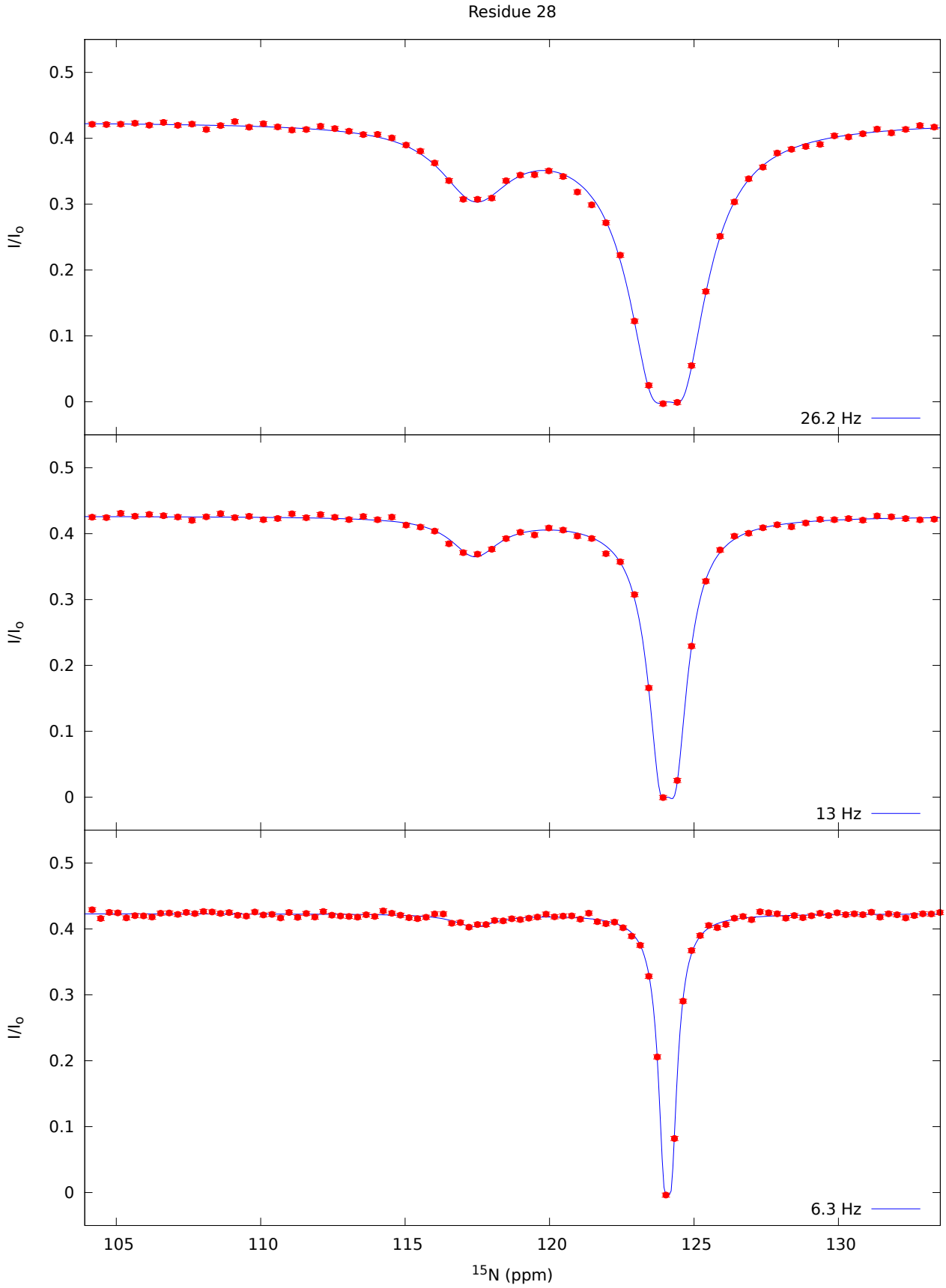
Residue 28
I/I$_o$
0.5
0.4
0.3
0.2
0.1
0
26.2 Hz
13 Hz
6.3 Hz
105
110
115
120
125
130
^{15}N (ppm)

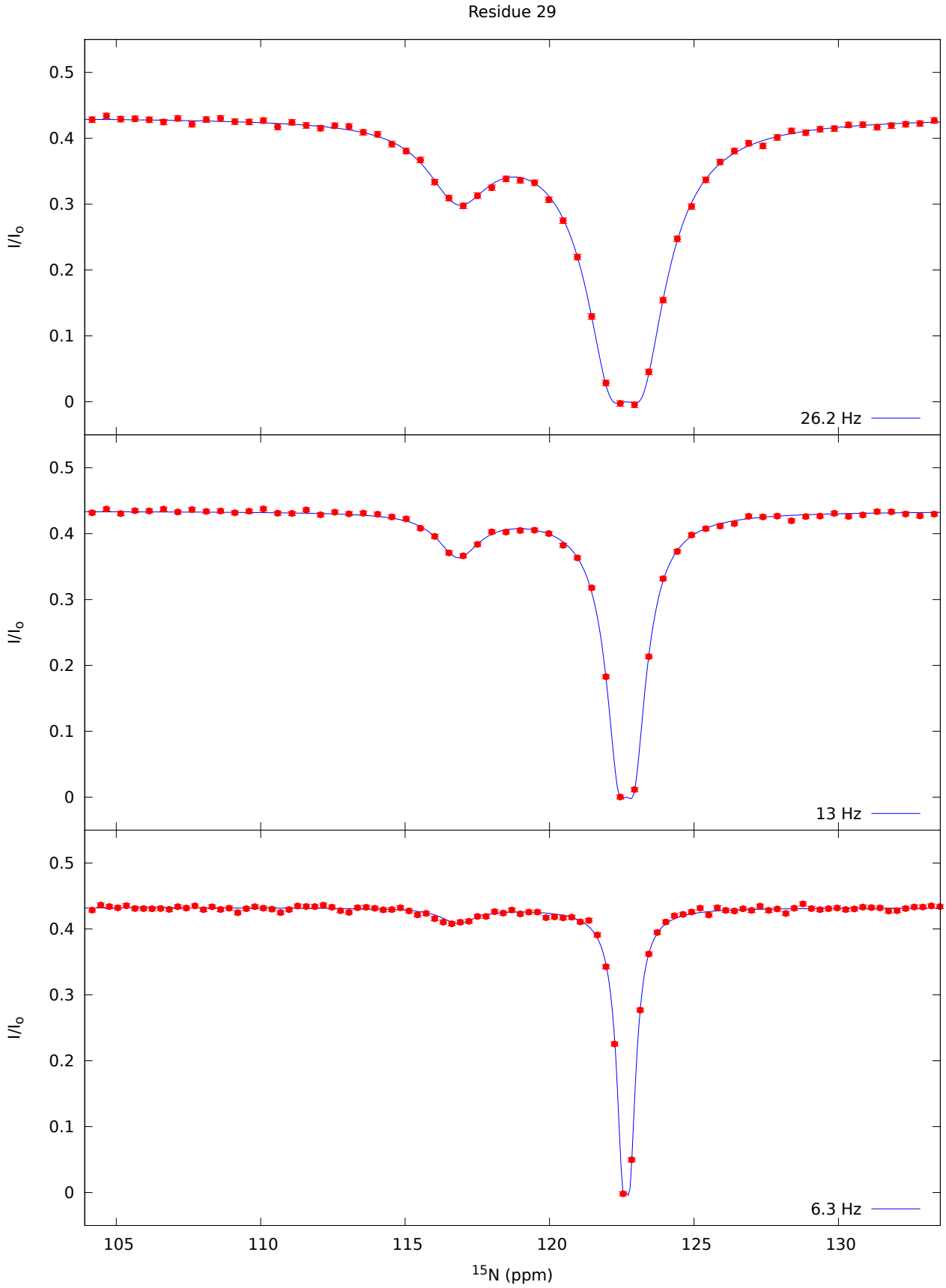
Residue 29
I/I$_o$
0.5
0.4
0.3
0.2
0.1
0
26.2 Hz
13 Hz
6.3 Hz
105
110
115
120
125
130
^{15}N (ppm)

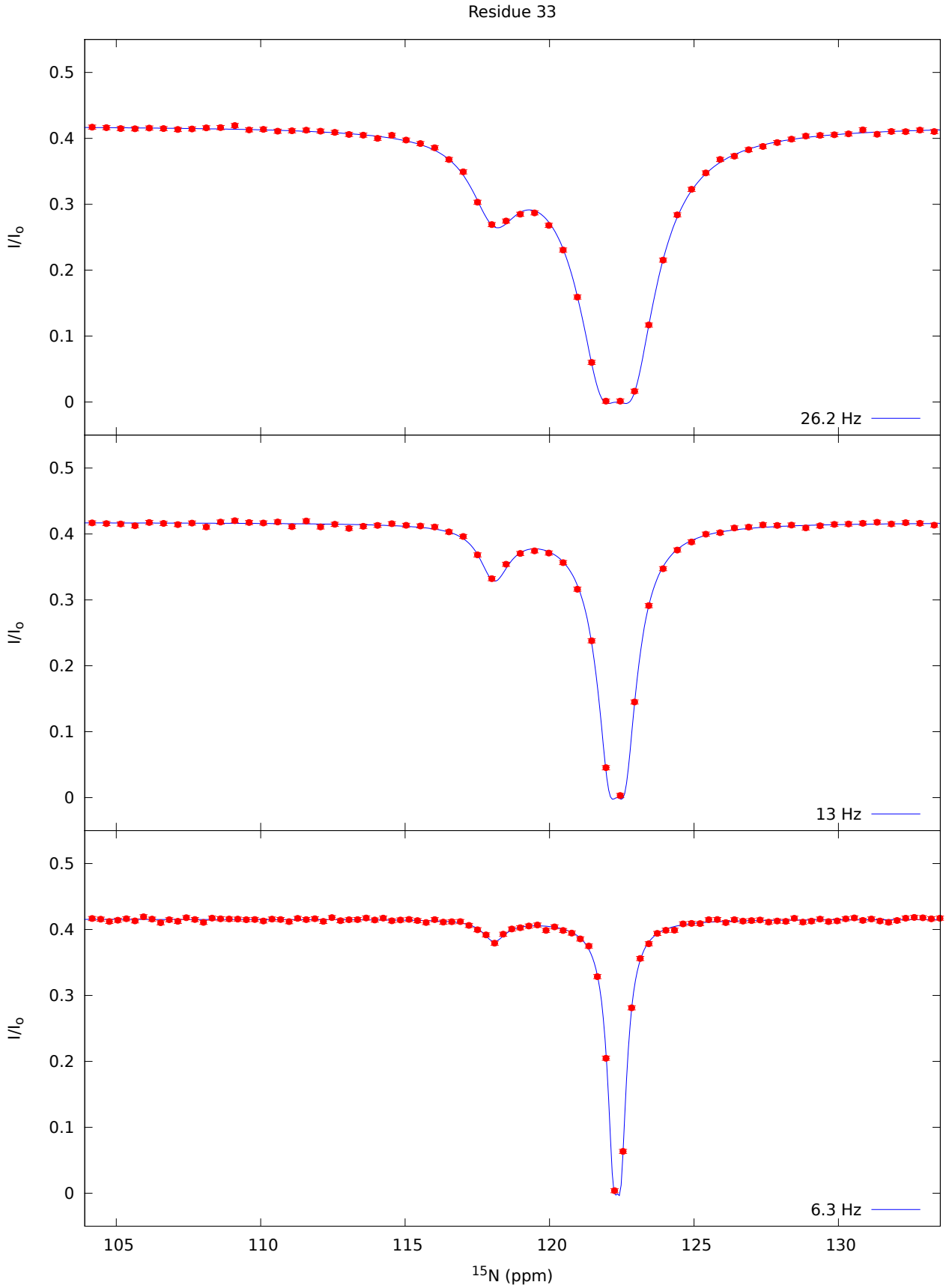
Residue 33
I/I$_o$
0.5
0.4
0.3
0.2
0.1
0
26.2 Hz
13 Hz
6.3 Hz
105
110
115
120
125
130
^{15}N (ppm)

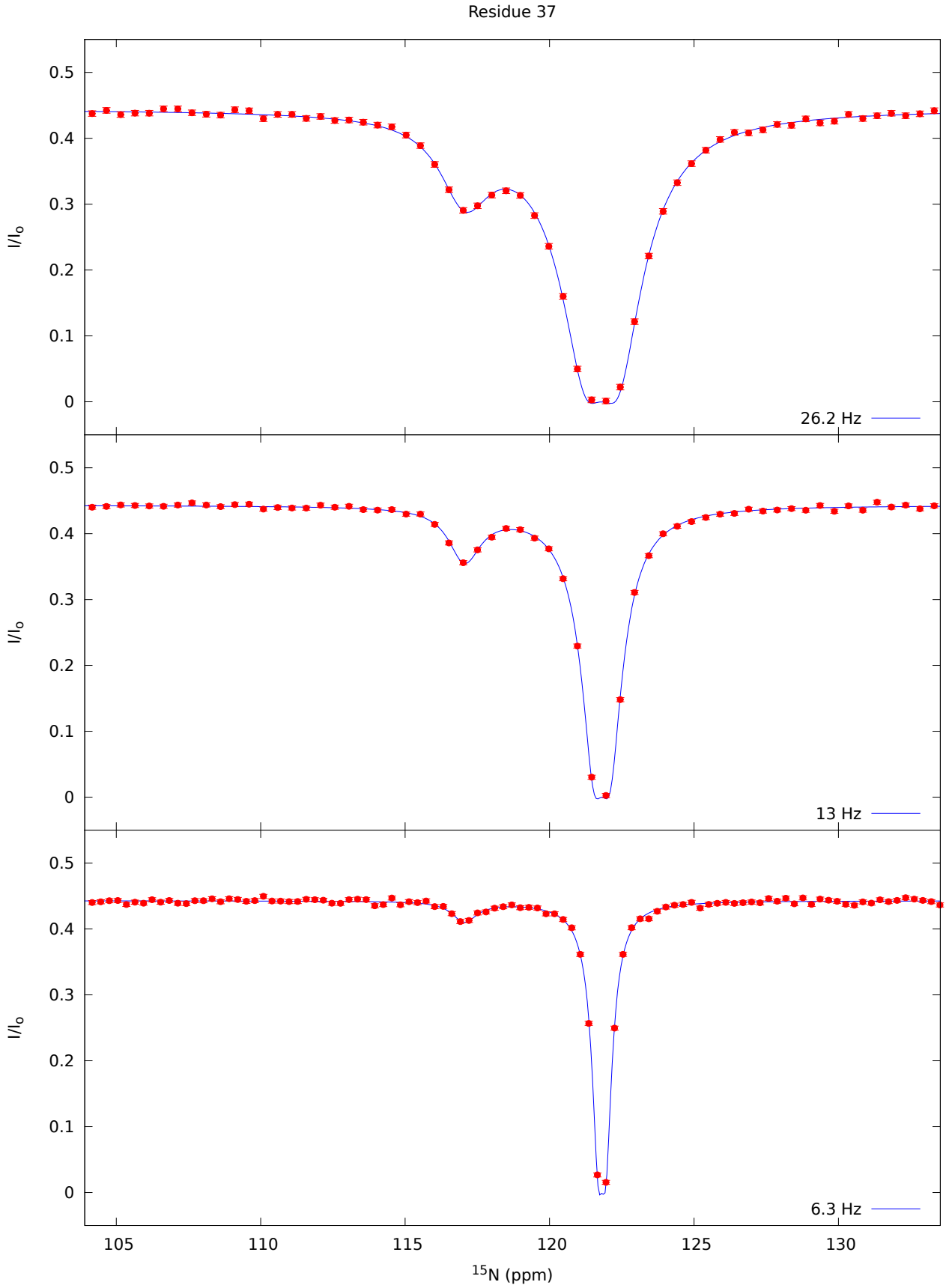
Residue 37
I/I$_o$
0.5
0.4
0.3
0.2
0.1
0
26.2 Hz
13 Hz
6.3 Hz
105
110
115
120
125
130
^{15}N (ppm)

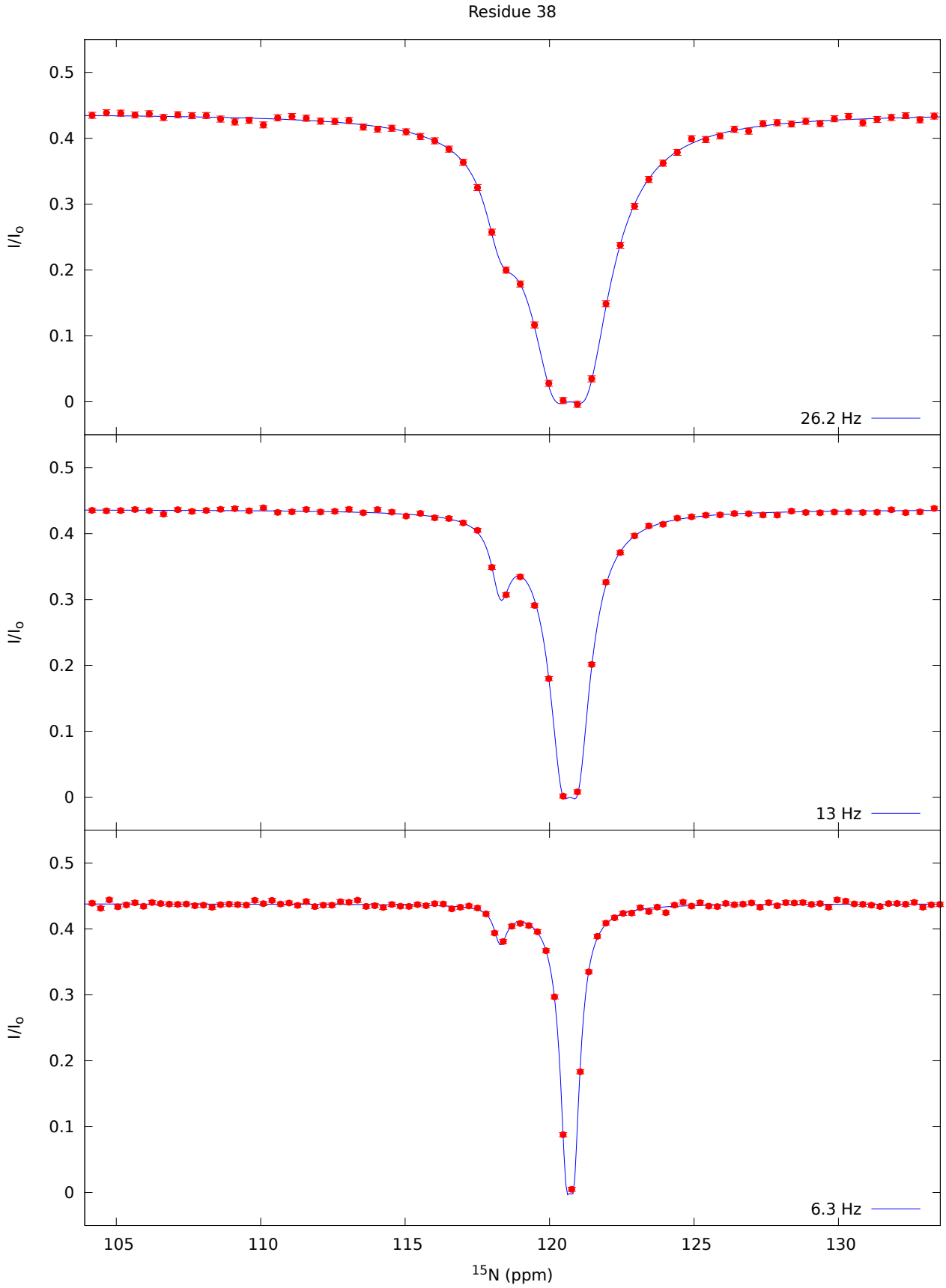
Residue 38
I/I$_o$
0.5
0.4
0.3
0.2
0.1
0
26.2 Hz
13 Hz
6.3 Hz
105
110
115
120
125
130
^{15}N (ppm)

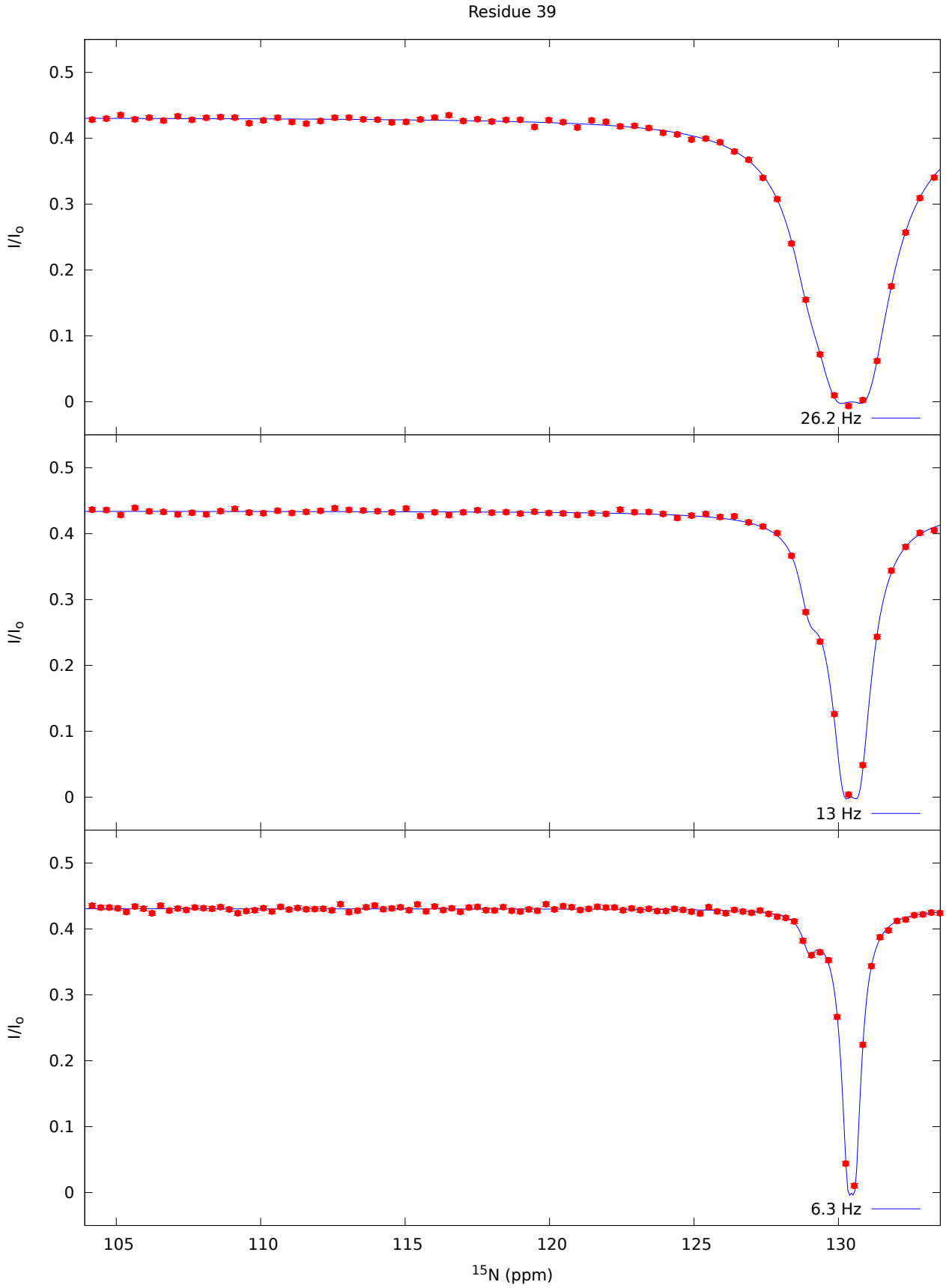
Residue 39
I/I$_o$
0.5
0.4
0.3
0.2
0.1
0
26.2 Hz
13 Hz
6.3 Hz
105
110
115
120
125
130
^{15}N (ppm)

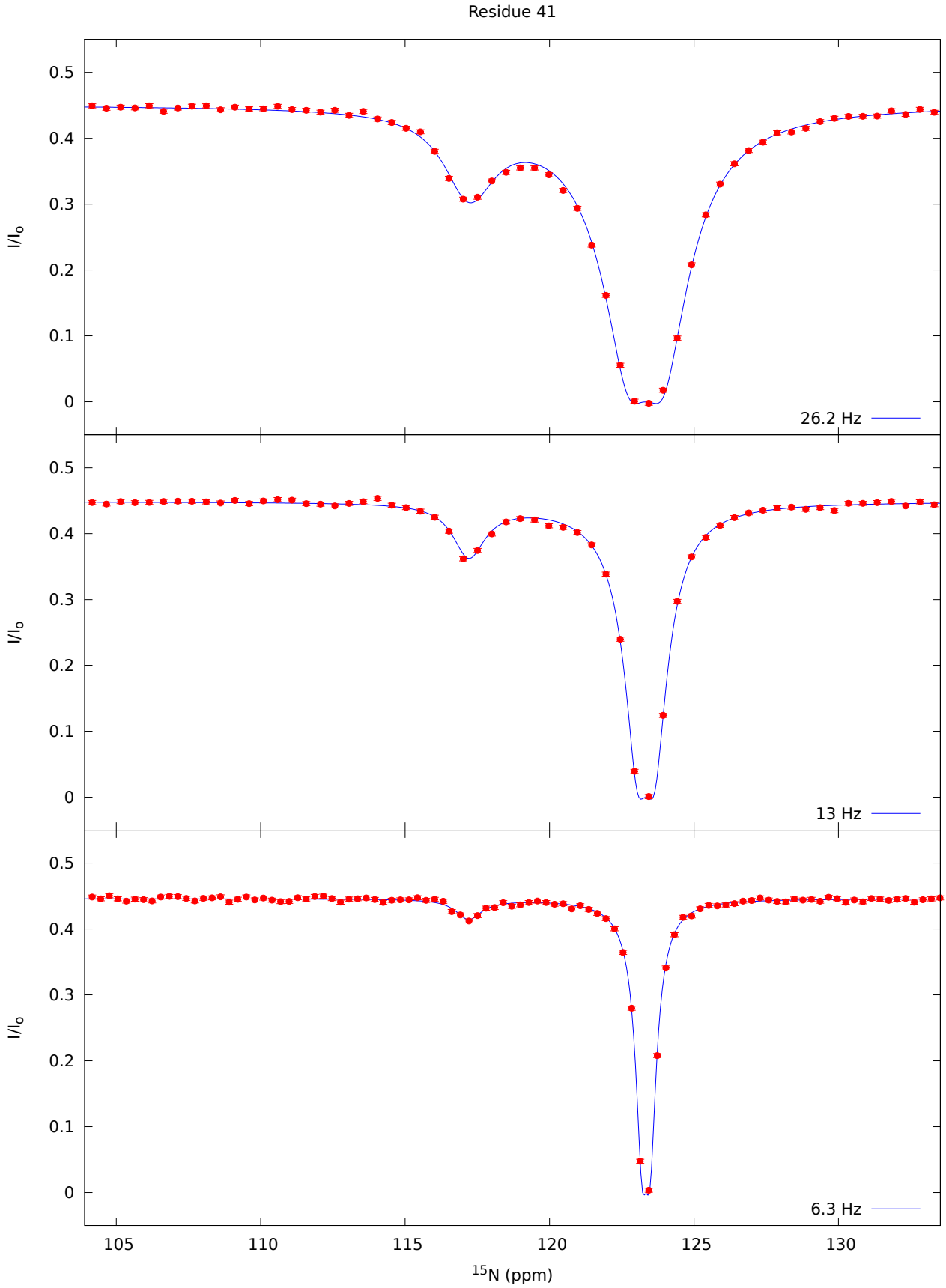
Residue 41
I/I$_o$
0.5
0.4
0.3
0.2
0.1
0
26.2 Hz
13 Hz
6.3 Hz
105
110
115
120
125
130
^{15}N (ppm)

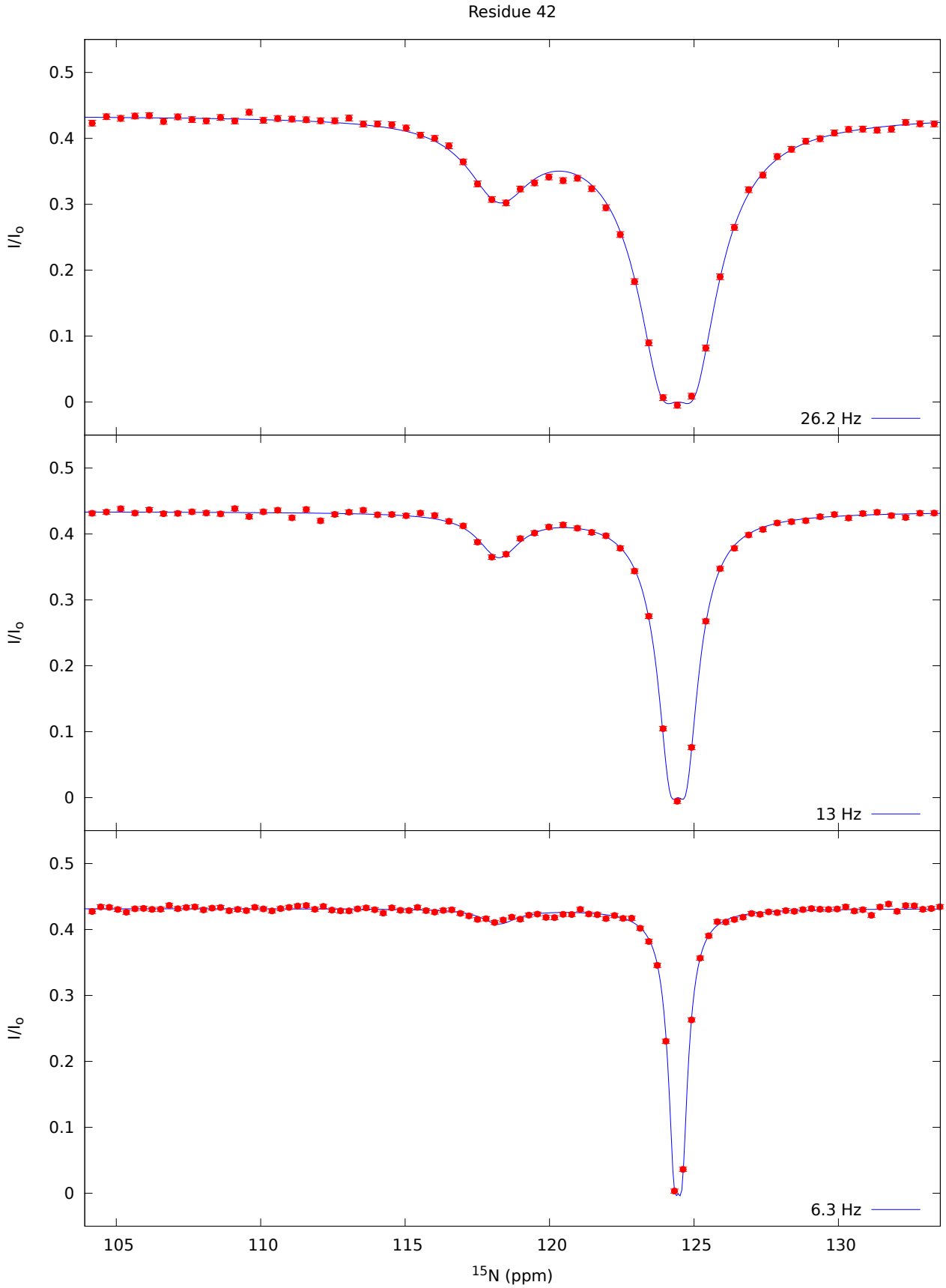
Residue 42
I/I$_o$
0.5
0.4
0.3
0.2
0.1
0
26.2 Hz
13 Hz
6.3 Hz
105
110
115
120
125
130
^{15}N (ppm)

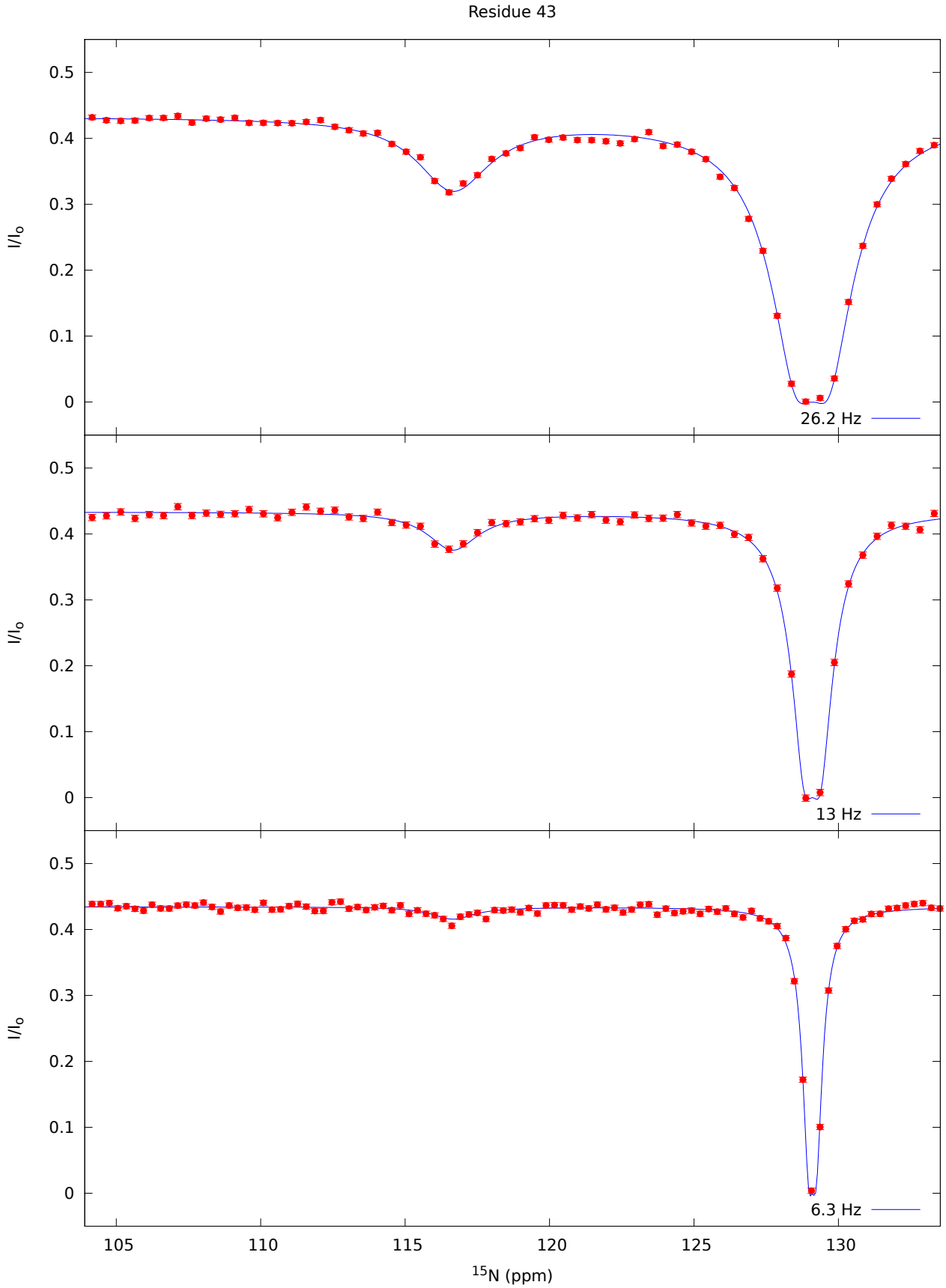
Residue 43
I/I$_o$
0.5
0.4
0.3
0.2
0.1
0
26.2 Hz
13 Hz
6.3 Hz
105
110
115
120
125
130
^{15}N (ppm)

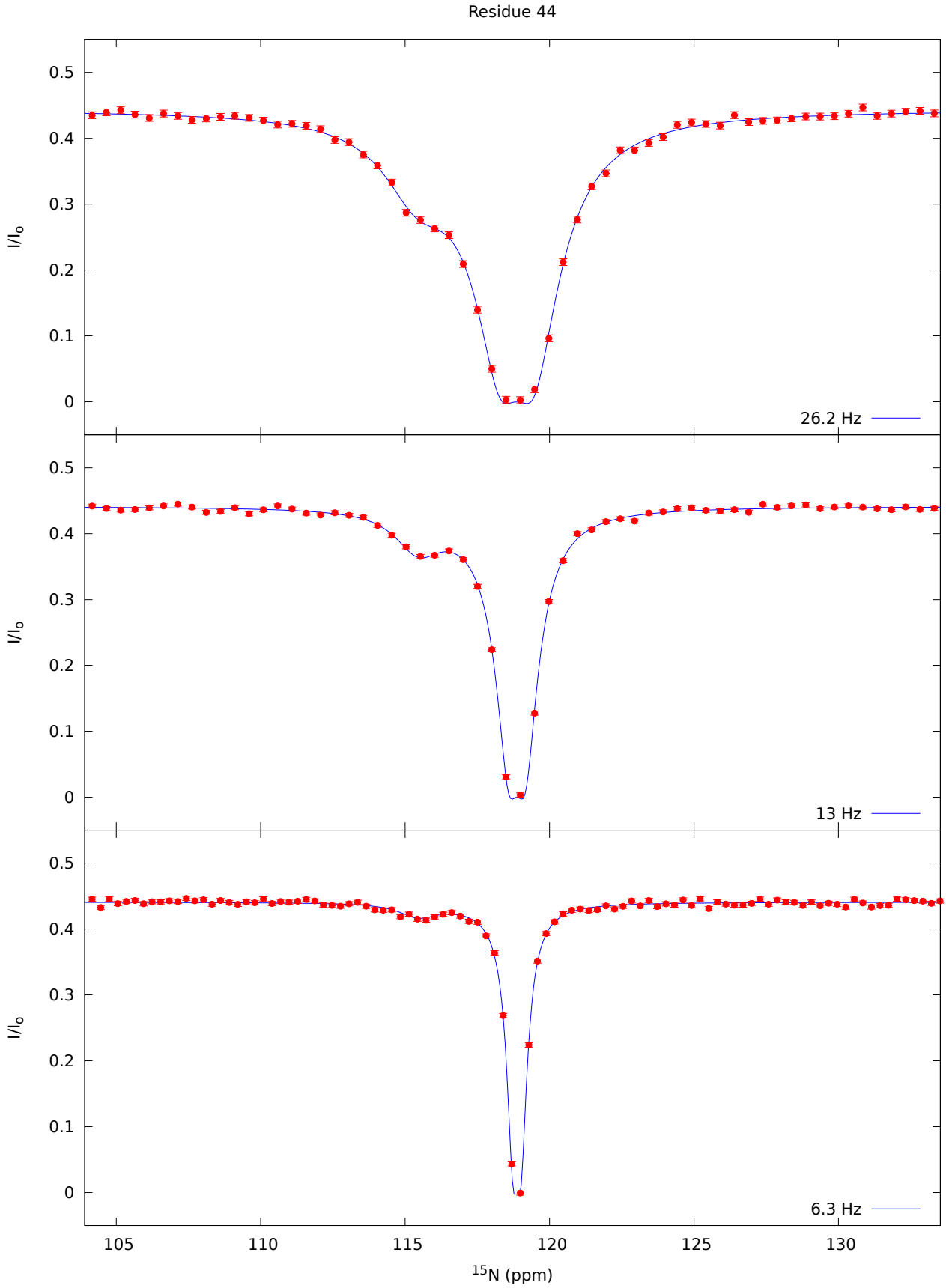
Residue 44
I/I$_o$
26.2 Hz
13 Hz
6.3 Hz
^{15}N (ppm)

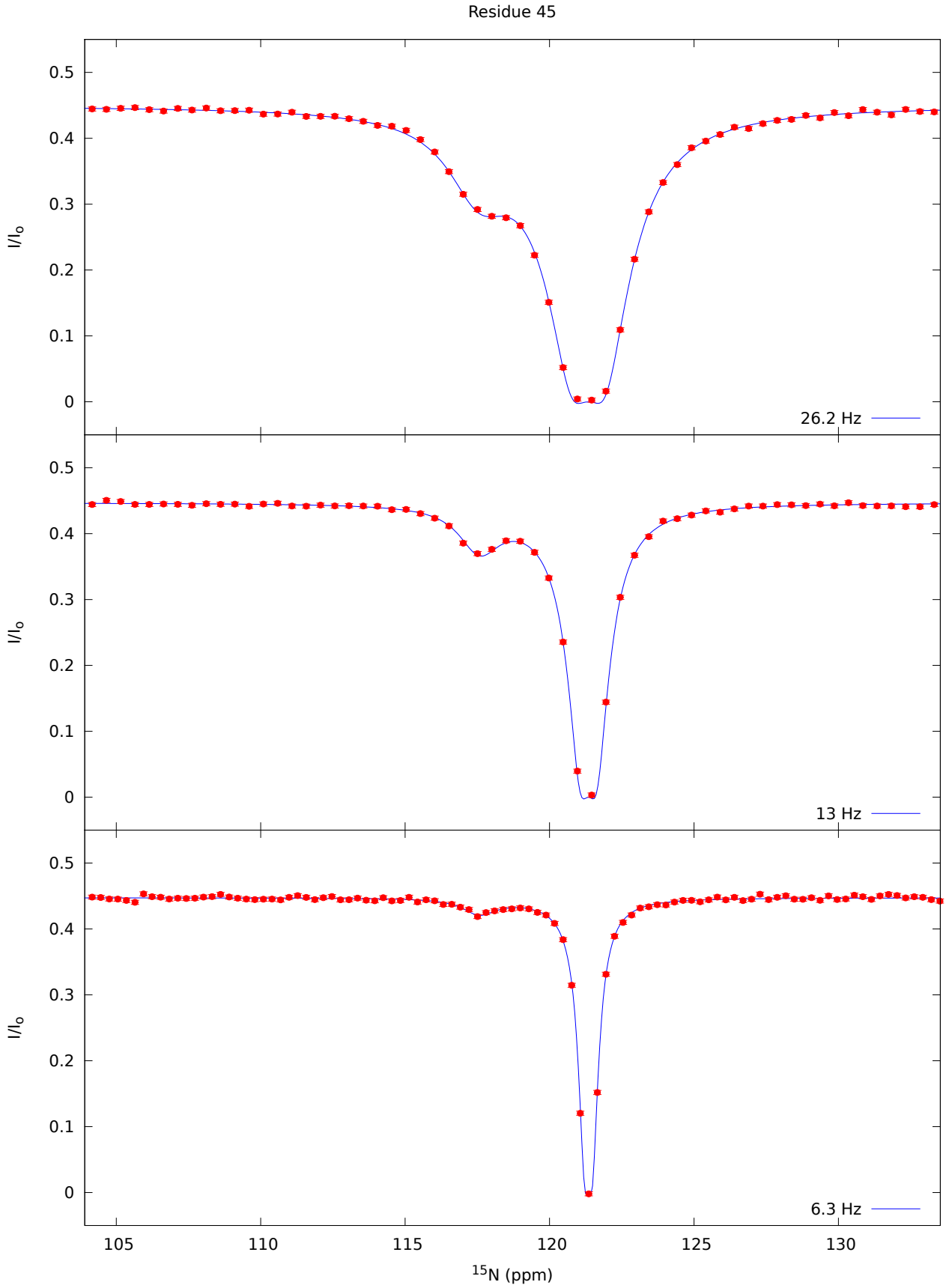
Residue 45
I/I$_o$
0.5
0.4
0.3
0.2
0.1
0
26.2 Hz
13 Hz
6.3 Hz
105
110
115
120
125
130
^{15}N (ppm)

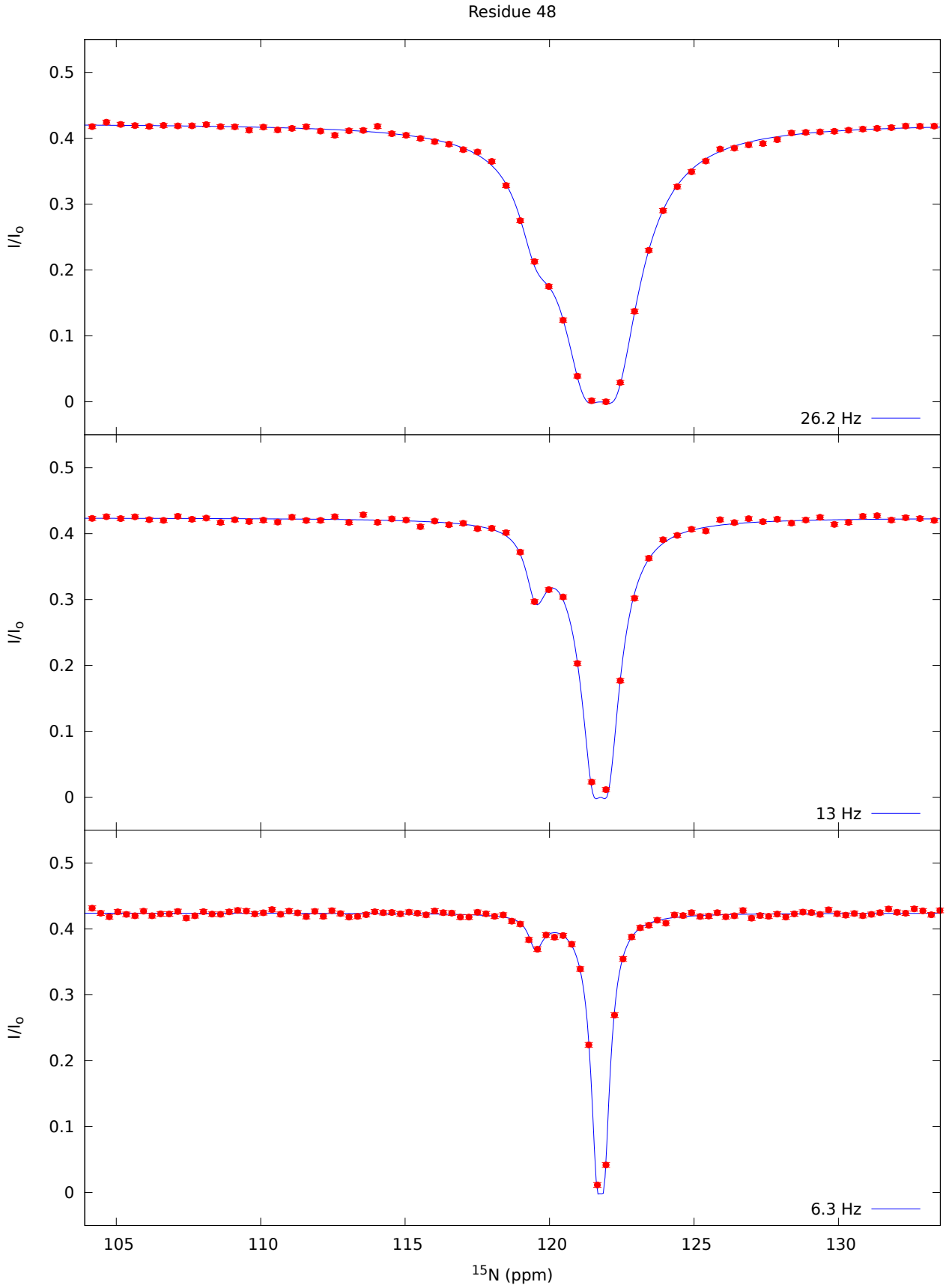
Residue 48
I/I$_o$
0.5
0.4
0.3
0.2
0.1
0
26.2 Hz
13 Hz
6.3 Hz
105
110
115
120
125
130
^{15}N (ppm)

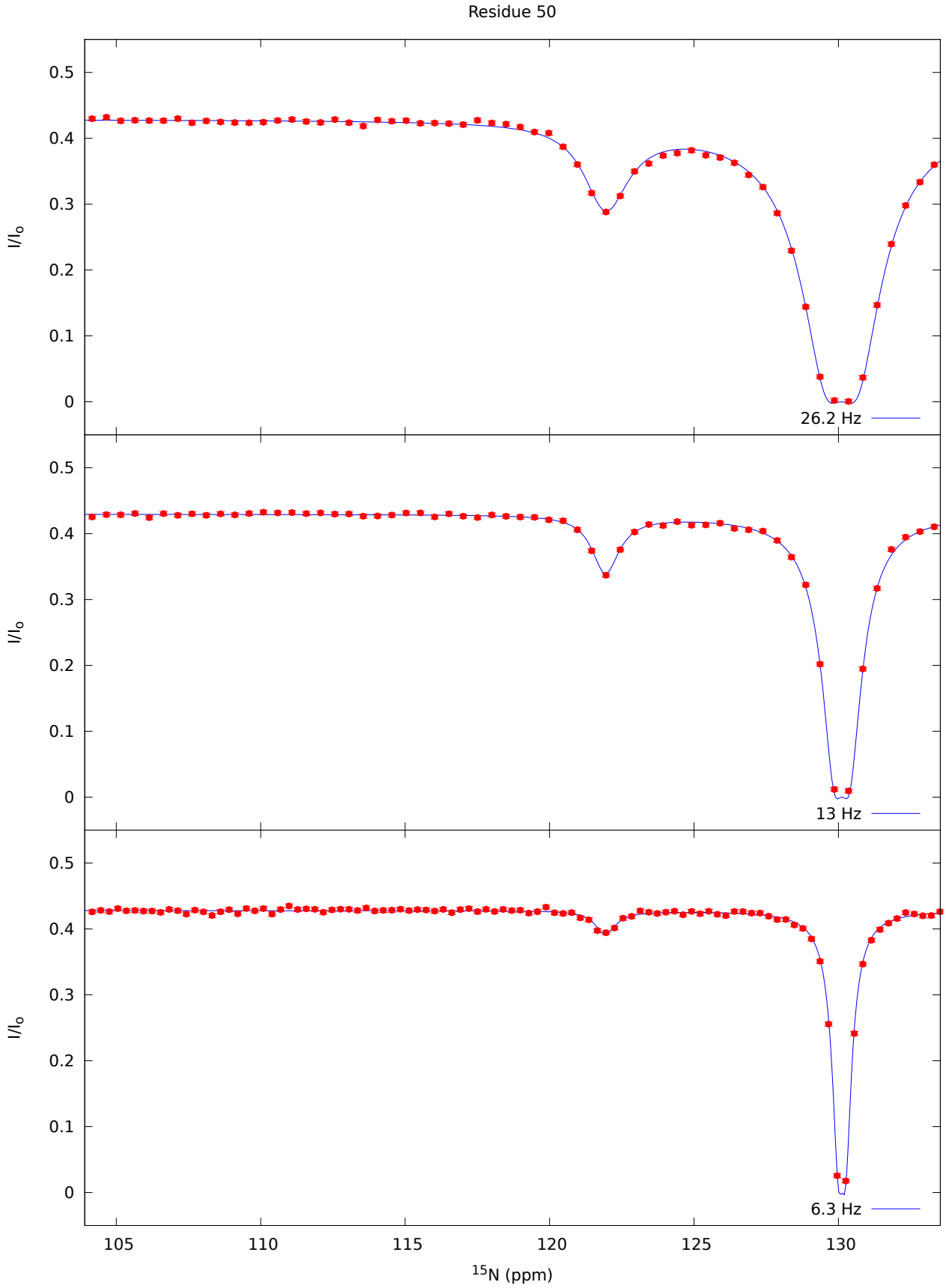
Residue 50
I/I$_o$
0.5
0.4
0.3
0.2
0.1
0
26.2 Hz
13 Hz
6.3 Hz
105
110
115
120
125
130
^{15}N (ppm)

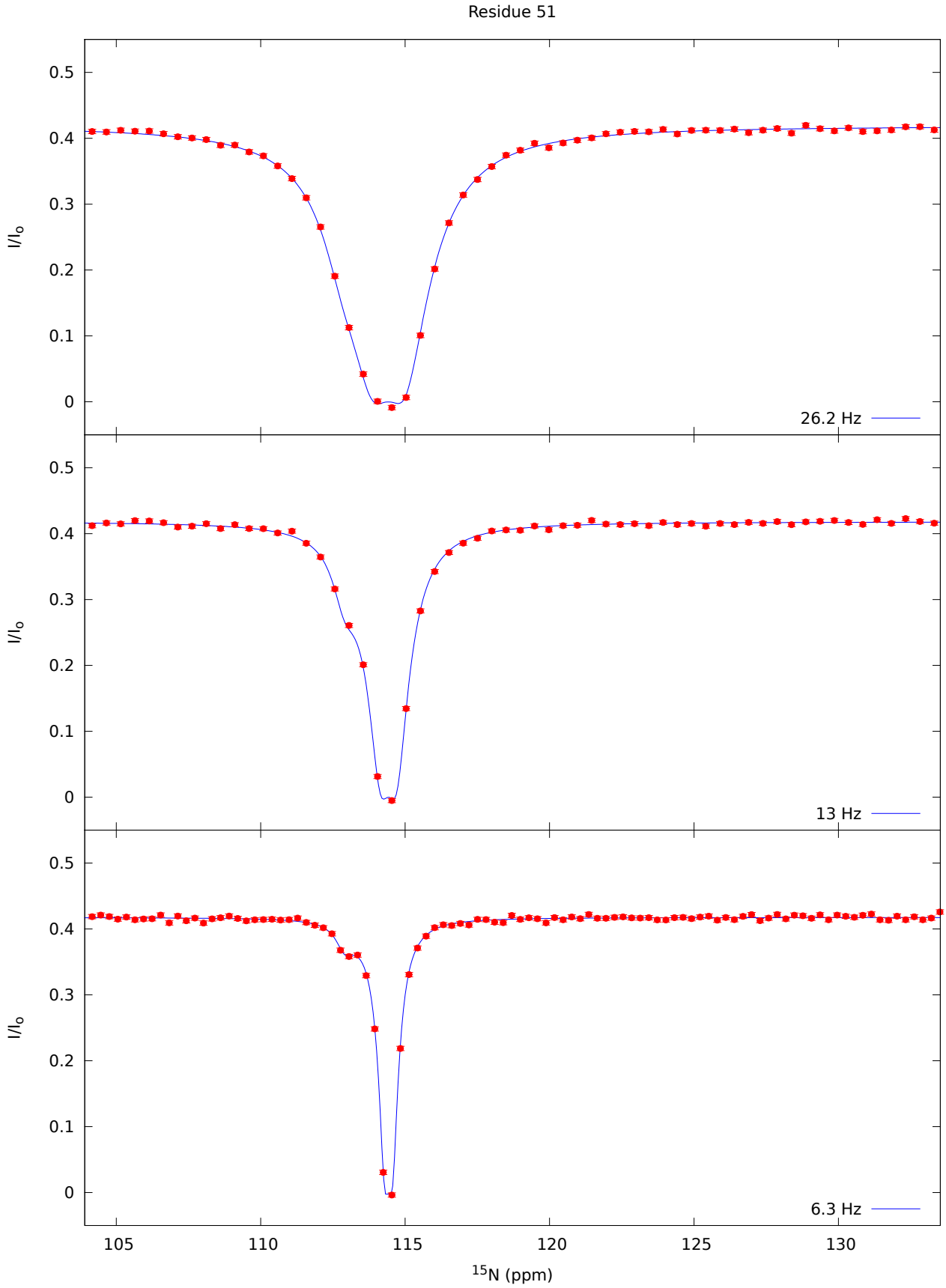
Residue 51
I/I$_o$
0.5
0.4
0.3
0.2
0.1
0
26.2 Hz
13 Hz
6.3 Hz
105
110
115
120
125
130
^{15}N (ppm)

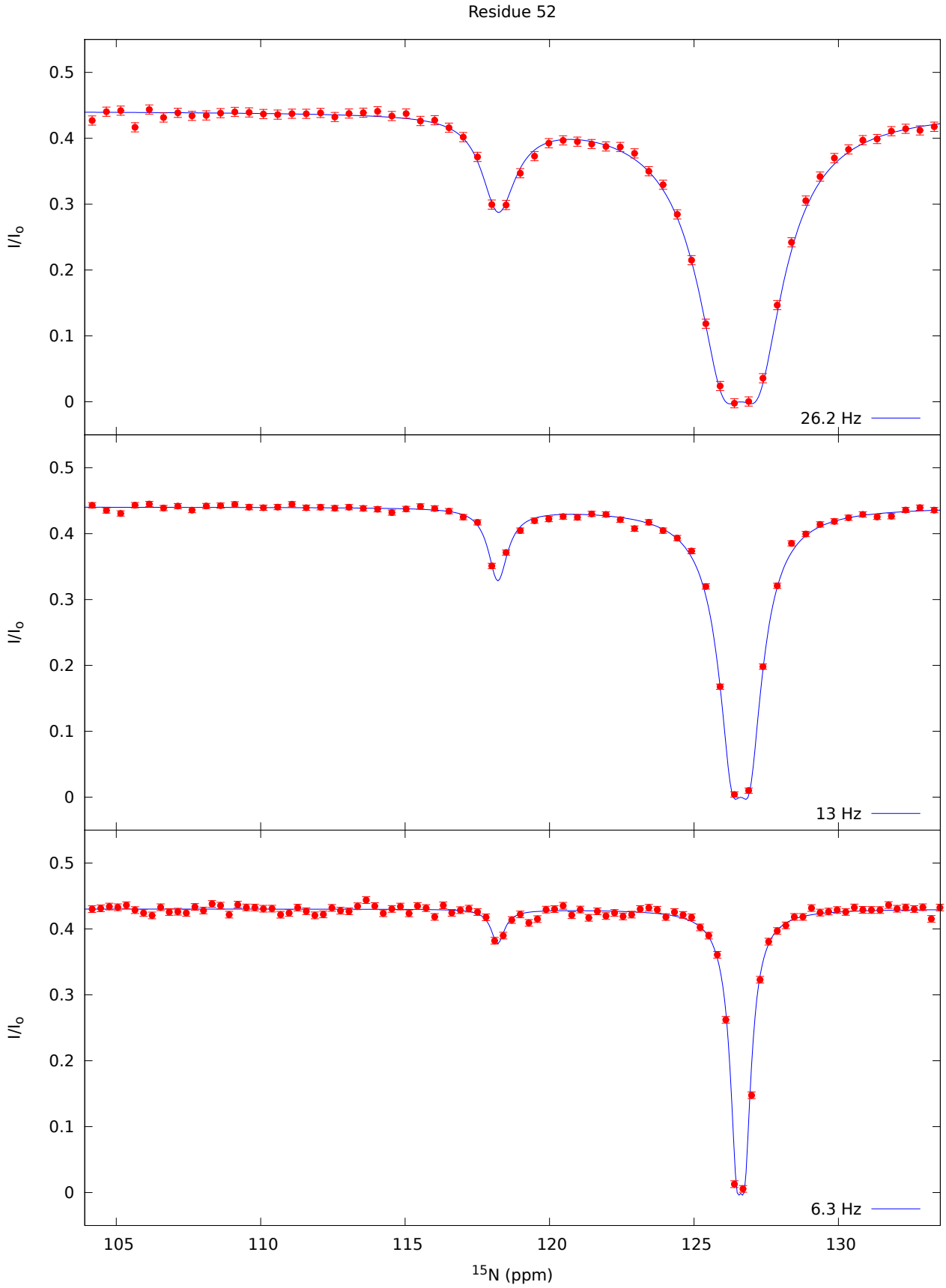
Residue 52
I/I$_o$
0.5
0.4
0.3
0.2
0.1
0
26.2 Hz
13 Hz
6.3 Hz
105
110
115
120
125
130
^{15}N (ppm)

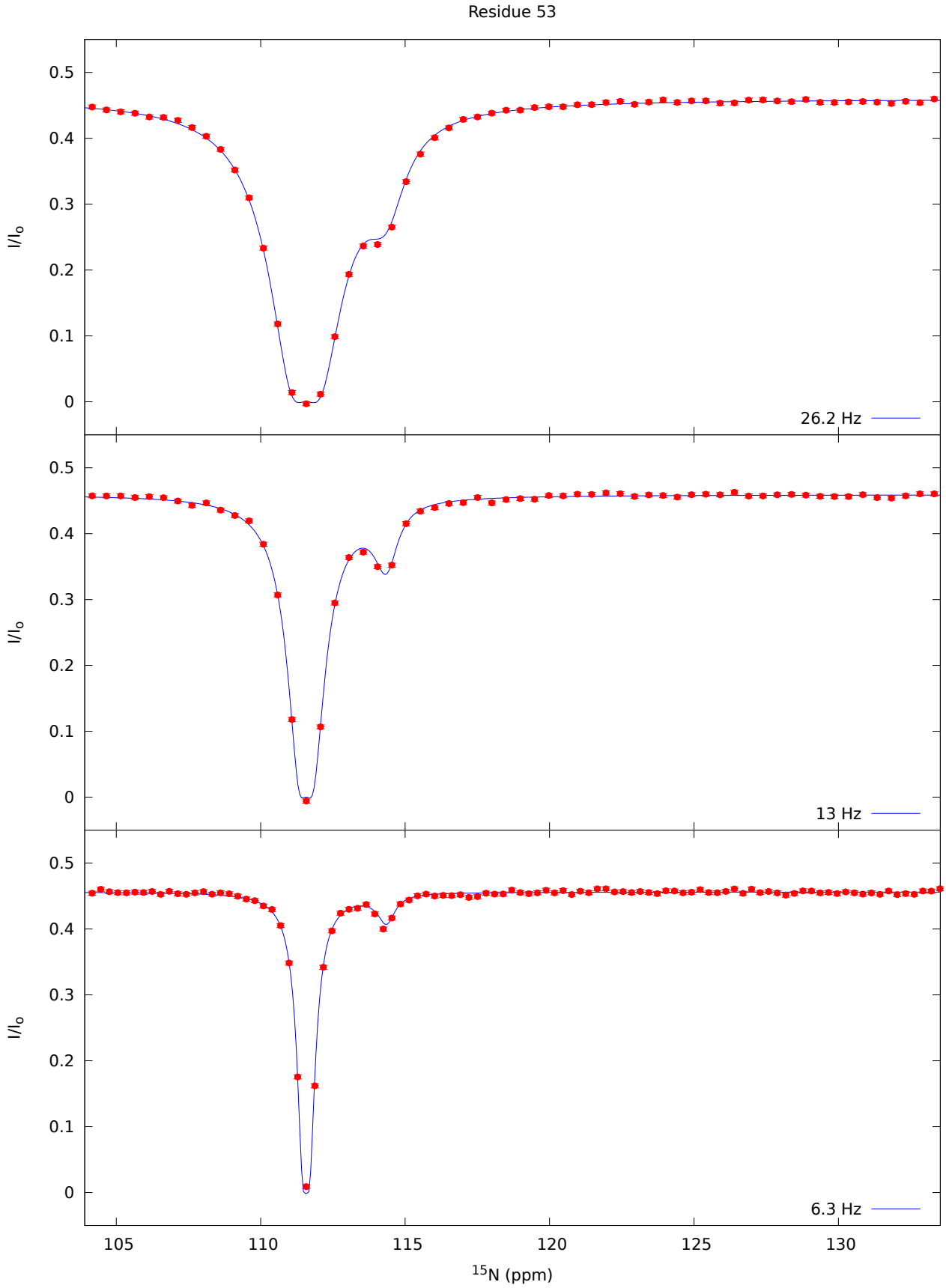
Residue 53
I/I$_o$
0.5
0.4
0.3
0.2
0.1
0
26.2 Hz
13 Hz
6.3 Hz
105
110
115
120
125
130
^{15}N (ppm)

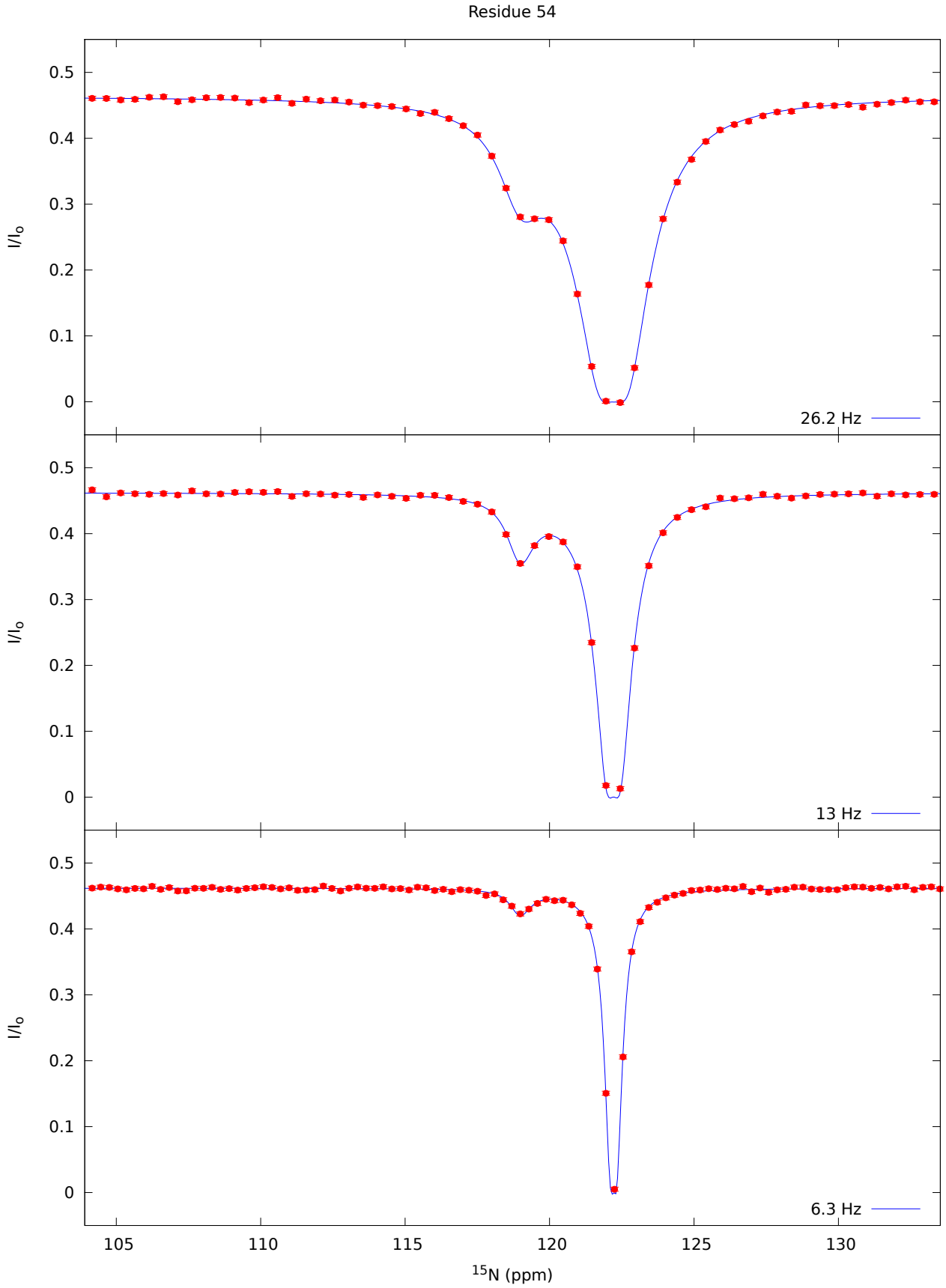
Residue 54
I/I$_o$
0.5
0.4
0.3
0.2
0.1
0
26.2 Hz
13 Hz
6.3 Hz
105
110
115
120
125
130
^{15}N (ppm)

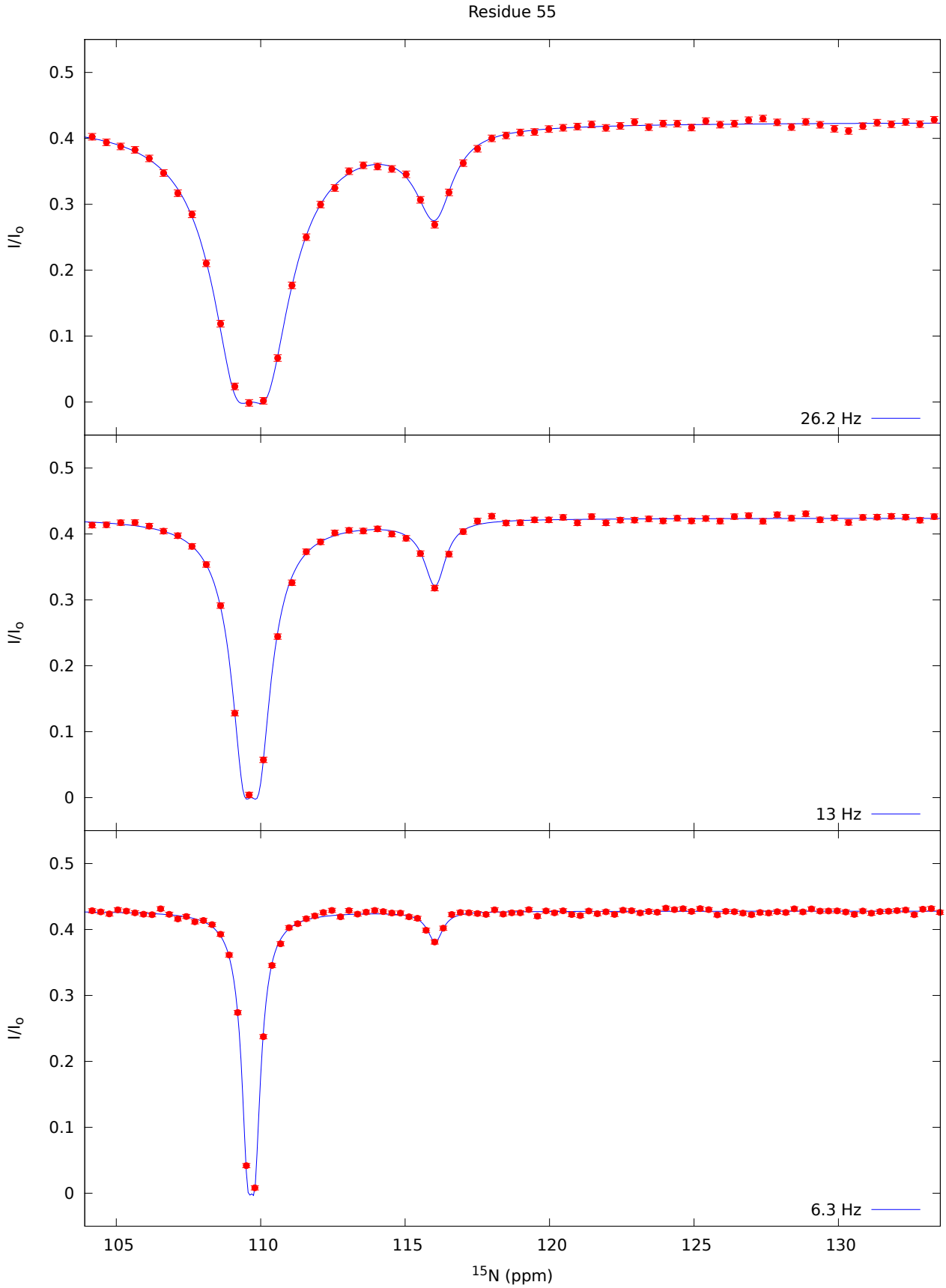
Residue 55
I/I$_o$
0.5
0.4
0.3
0.2
0.1
0
26.2 Hz
13 Hz
6.3 Hz
105
110
115
120
125
130
^{15}N (ppm)

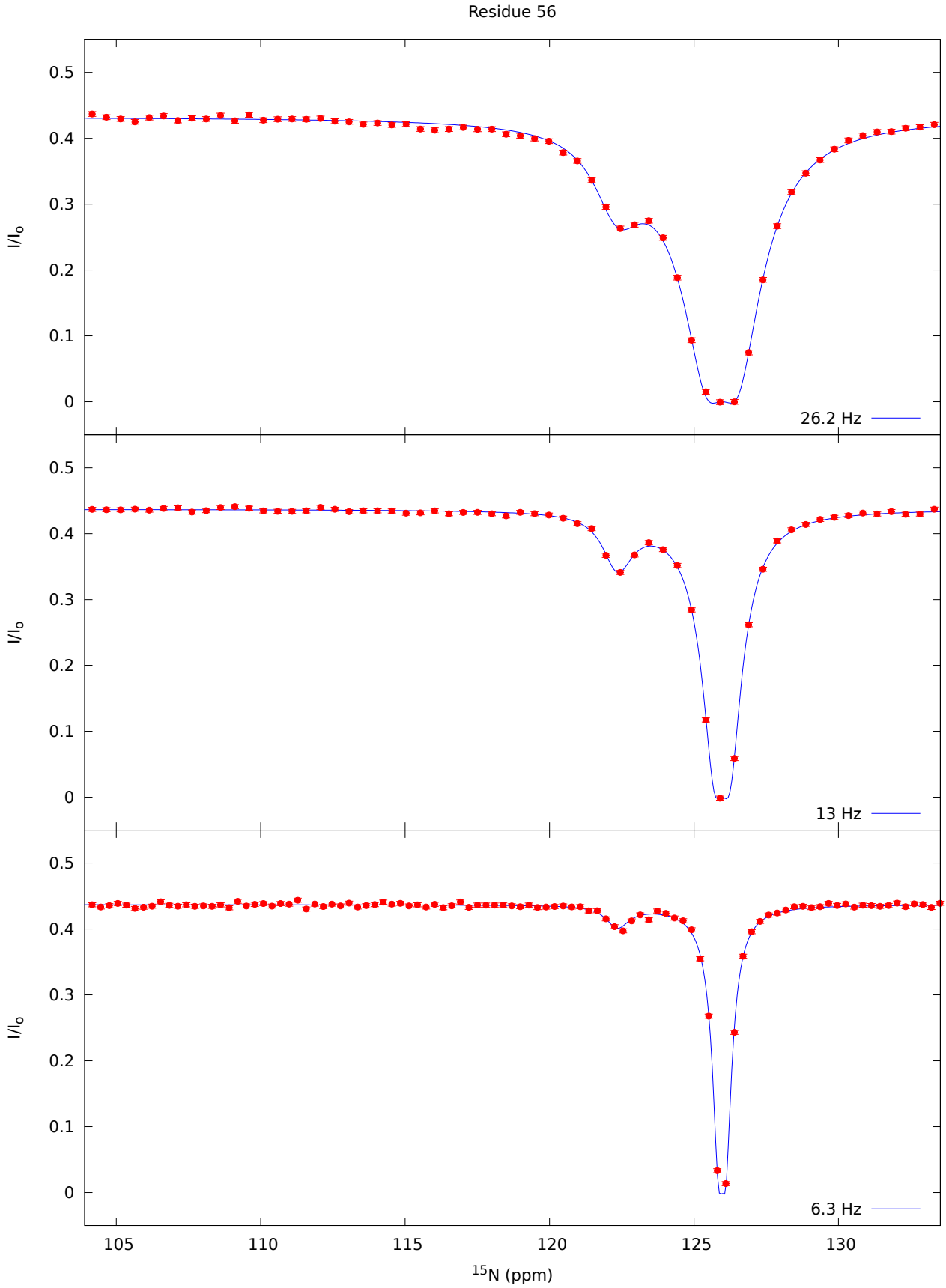
Residue 56
I/I$_o$
0.5
0.4
0.3
0.2
0.1
0
26.2 Hz
13 Hz
6.3 Hz
105
110
115
120
125
130
^{15}N (ppm)

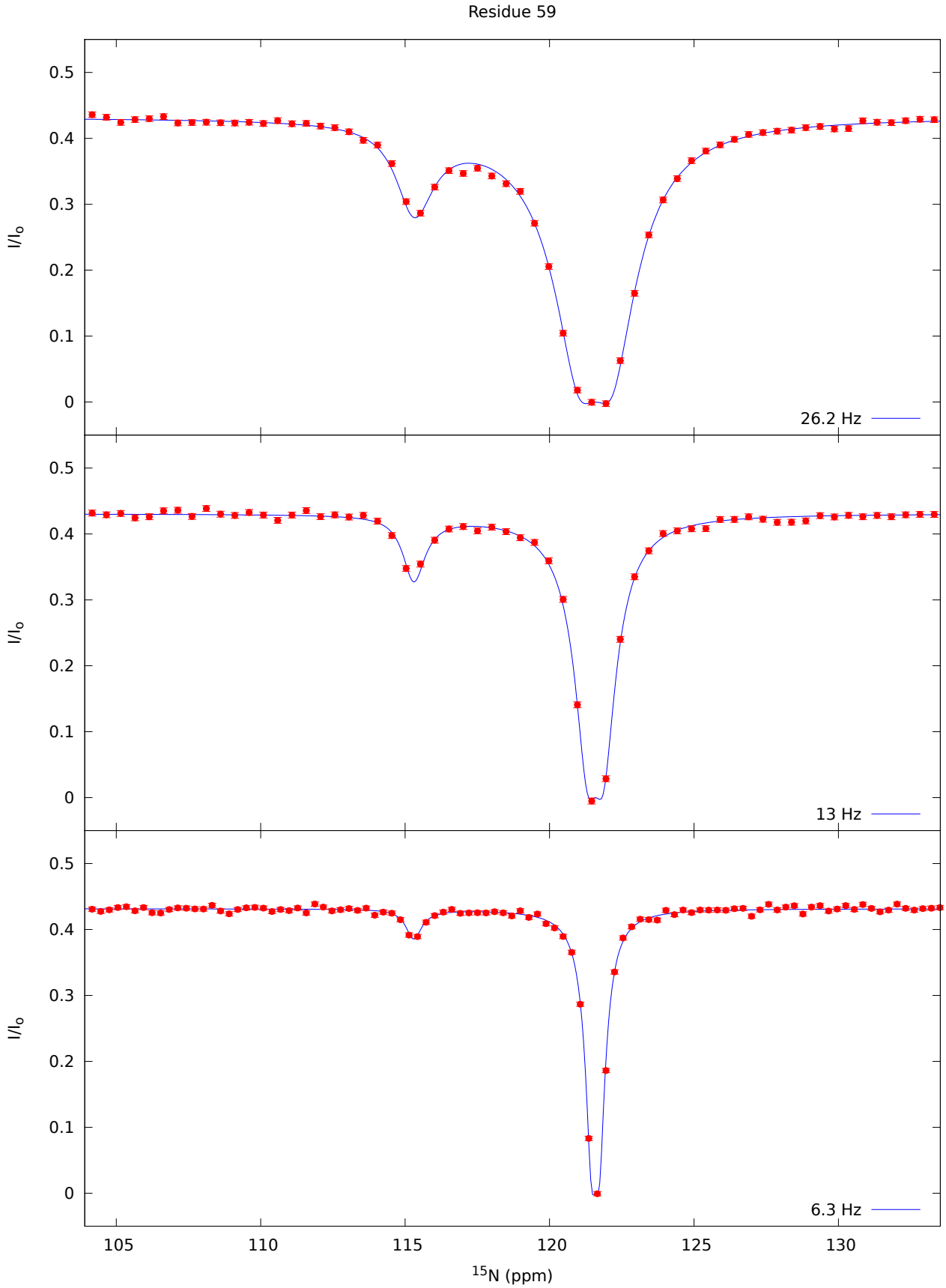
Residue 59
I/I$_o$
0.5
0.4
0.3
0.2
0.1
0
26.2 Hz
13 Hz
6.3 Hz
105
110
115
120
125
130
^{15}N (ppm)

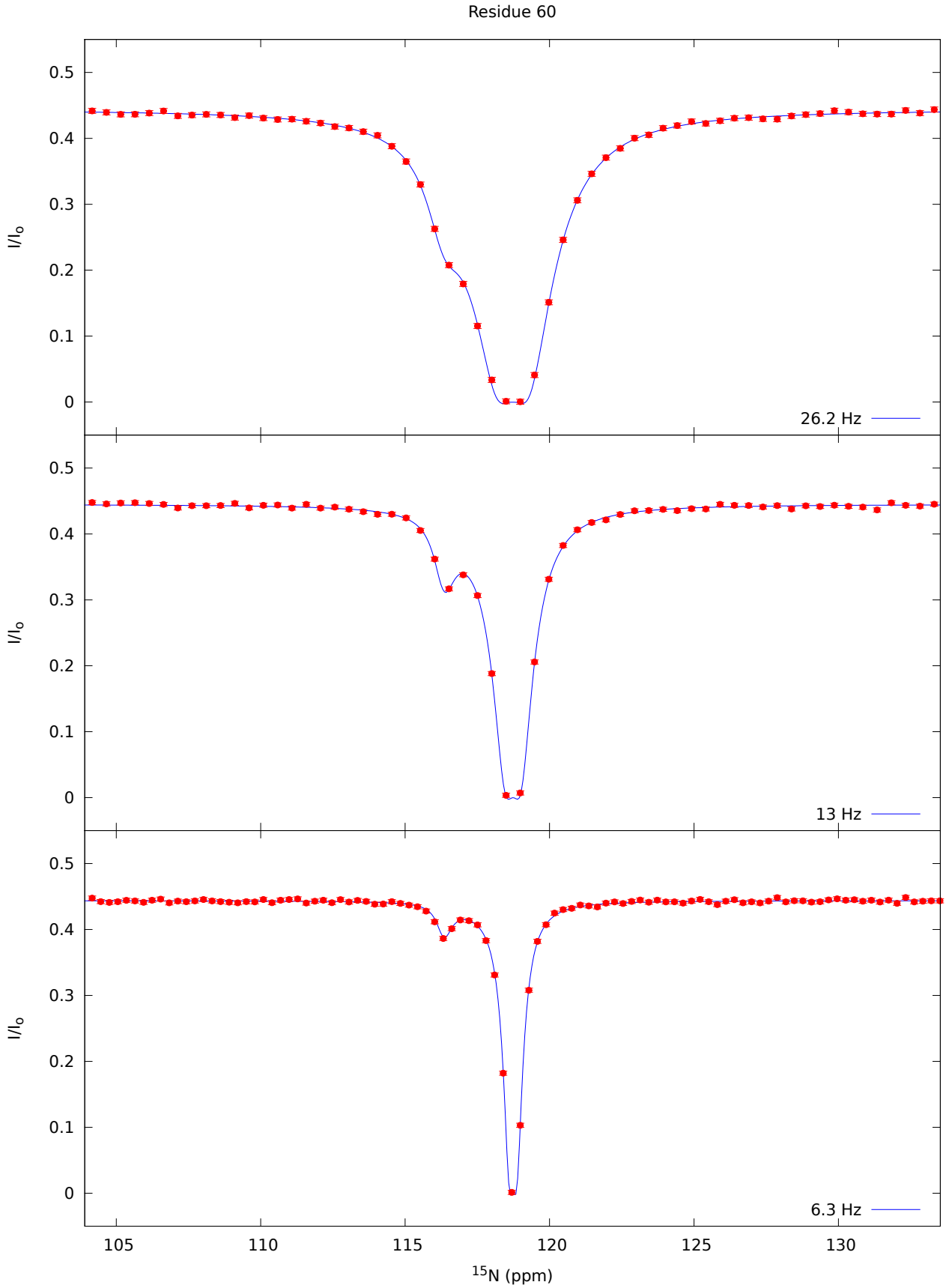
Residue 60
I/I$_o$
0.5
0.4
0.3
0.2
0.1
0
26.2 Hz
13 Hz
6.3 Hz
105
110
115
120
125
130
^{15}N (ppm)

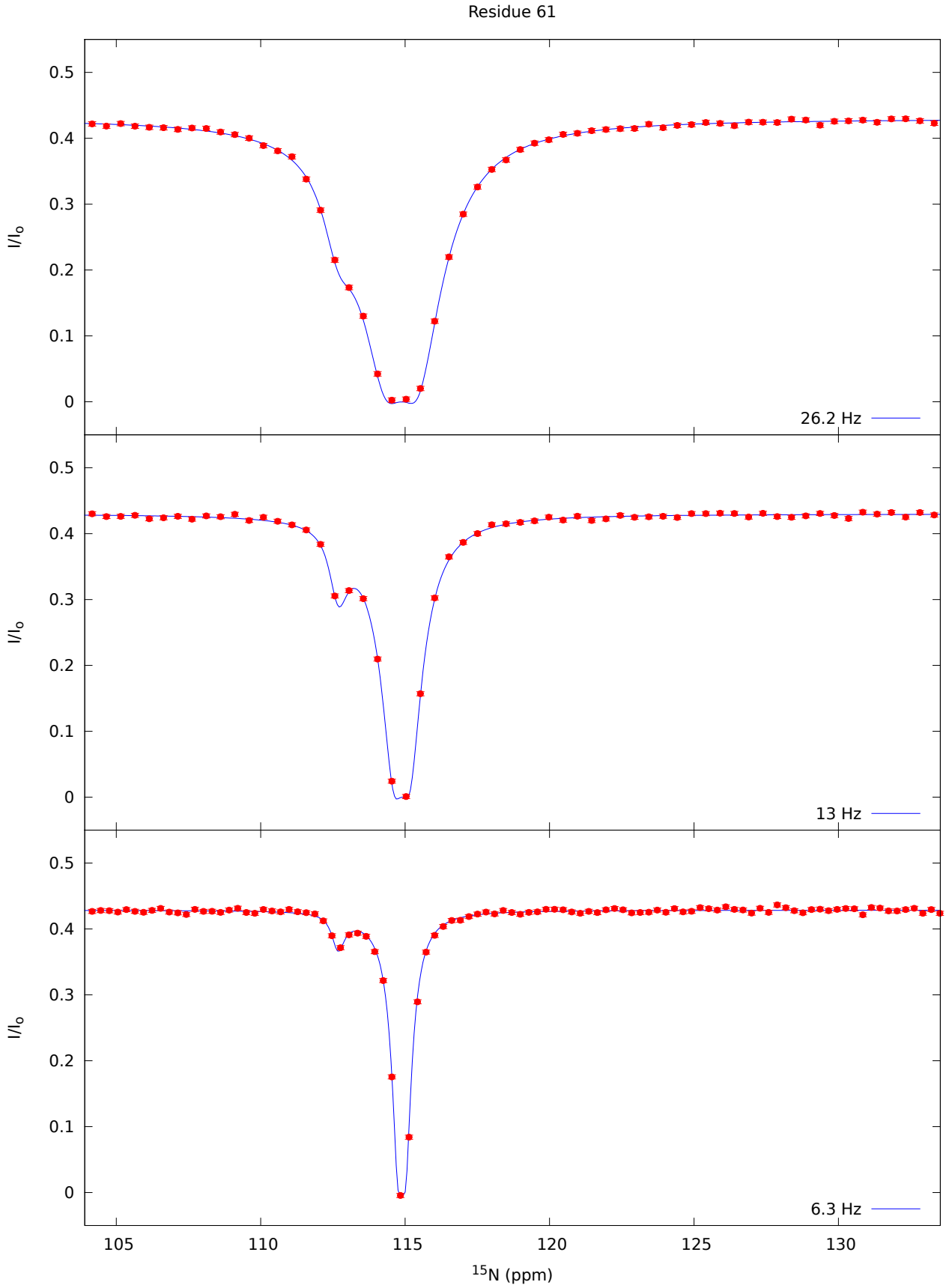
Residue 61
I/I$_o$
0.5
0.4
0.3
0.2
0.1
0
26.2 Hz
13 Hz
6.3 Hz
105
110
115
120
125
130
^{15}N (ppm)

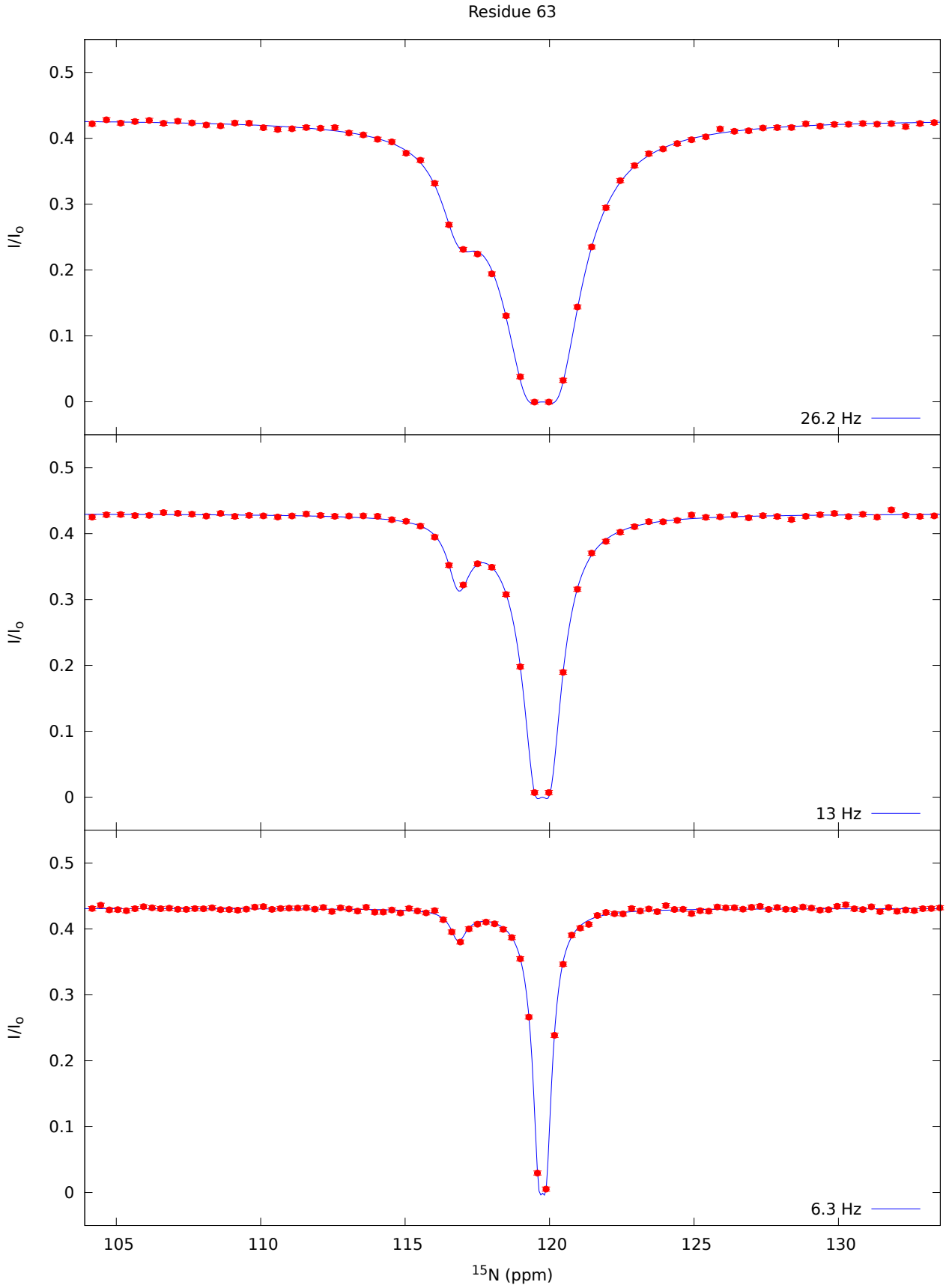
Residue 63
I/I$_o$
0.5
0.4
0.3
0.2
0.1
0
26.2 Hz
13 Hz
6.3 Hz
105
110
115
120
125
130
^{15}N (ppm)

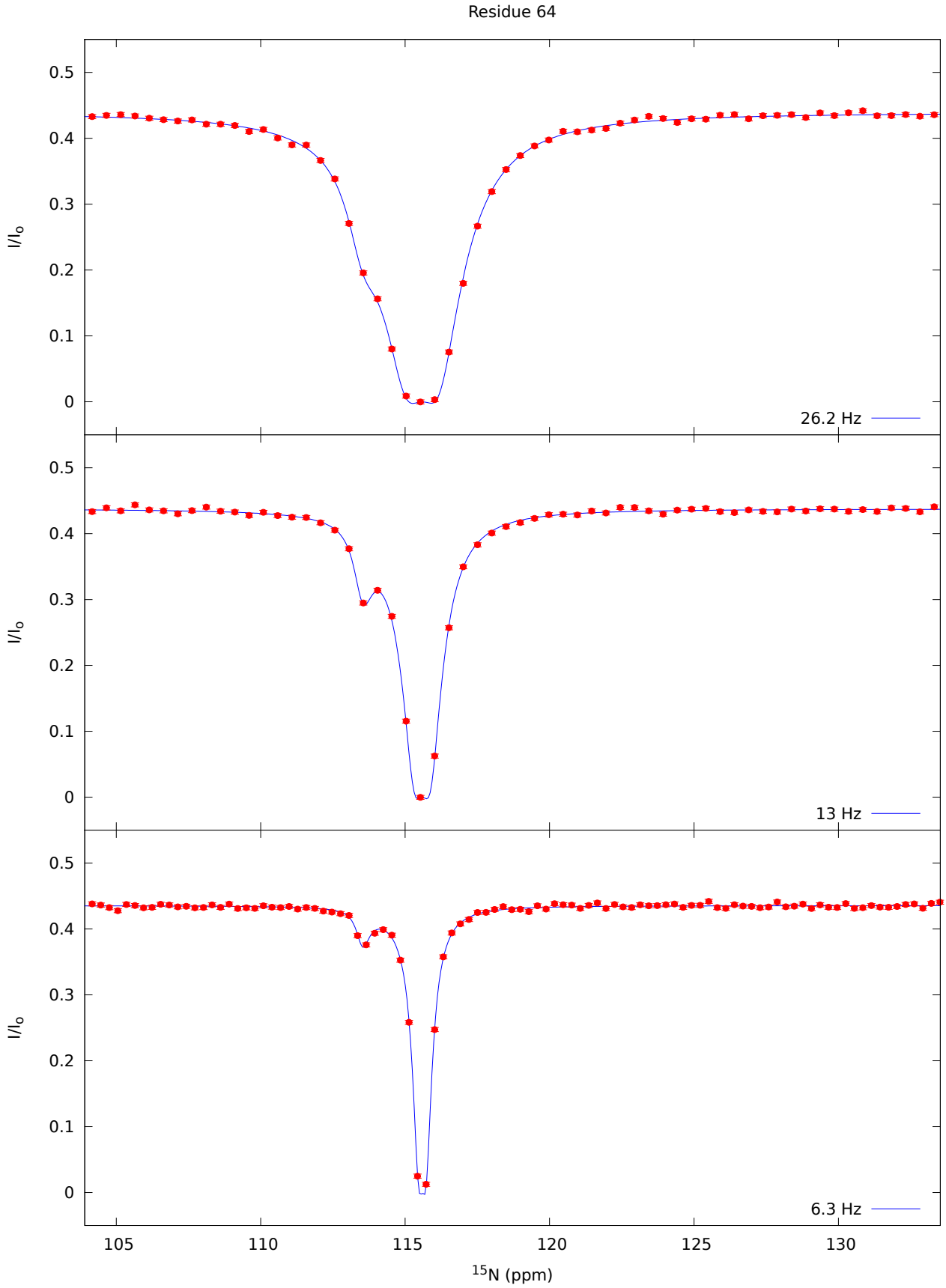
Residue 64
I/I$_o$
0.5
0.4
0.3
0.2
0.1
0
26.2 Hz
13 Hz
6.3 Hz
105
110
115
120
125
130
^{15}N (ppm)

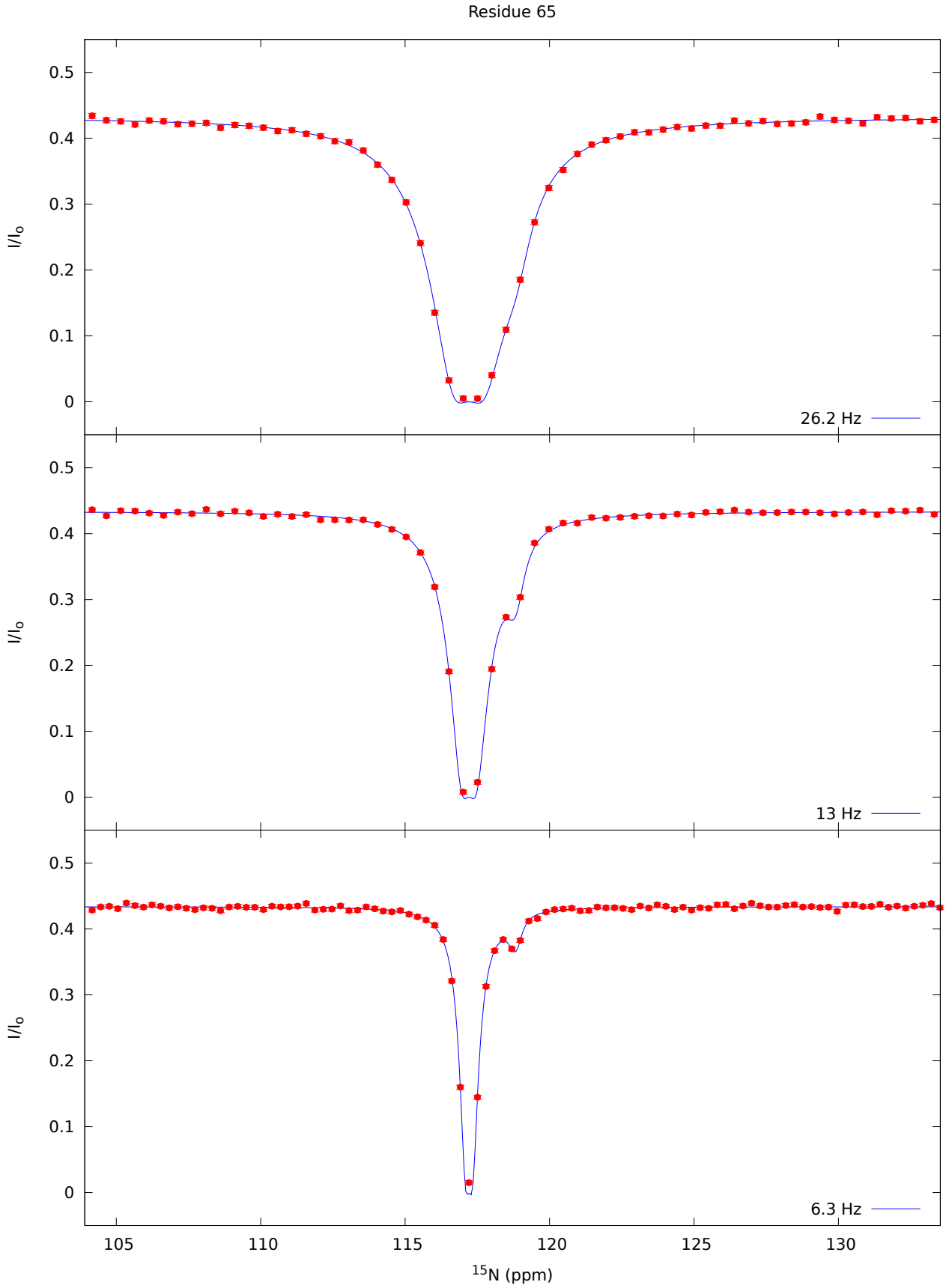
Residue 65
I/I$_o$
0.5
0.4
0.3
0.2
0.1
0
26.2 Hz
13 Hz
6.3 Hz
105
110
115
120
125
130
^{15}N (ppm)

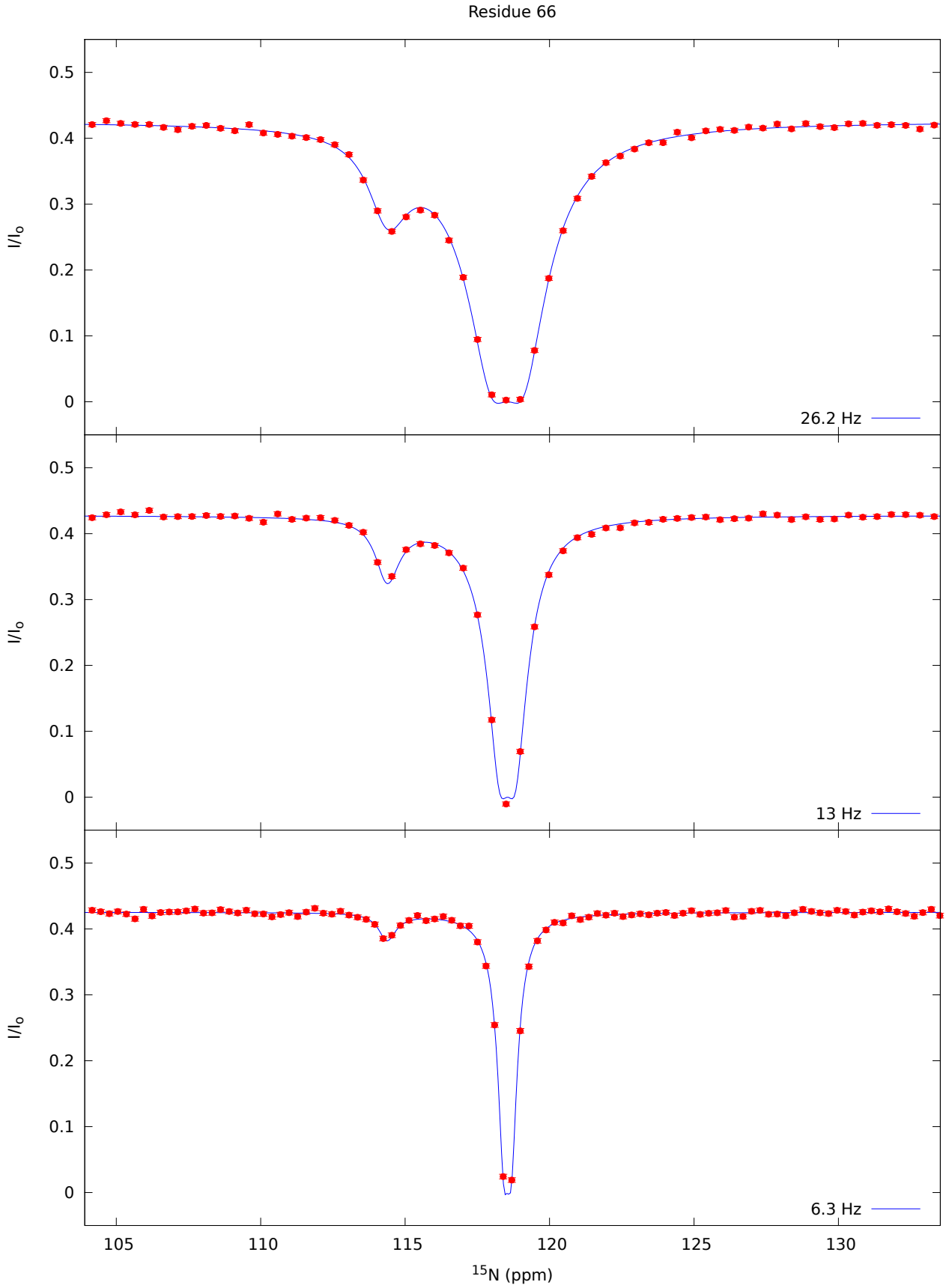
Residue 66
I/I$_o$
0.5
0.4
0.3
0.2
0.1
0
26.2 Hz
13 Hz
6.3 Hz
105
110
115
120
125
130
^{15}N (ppm)

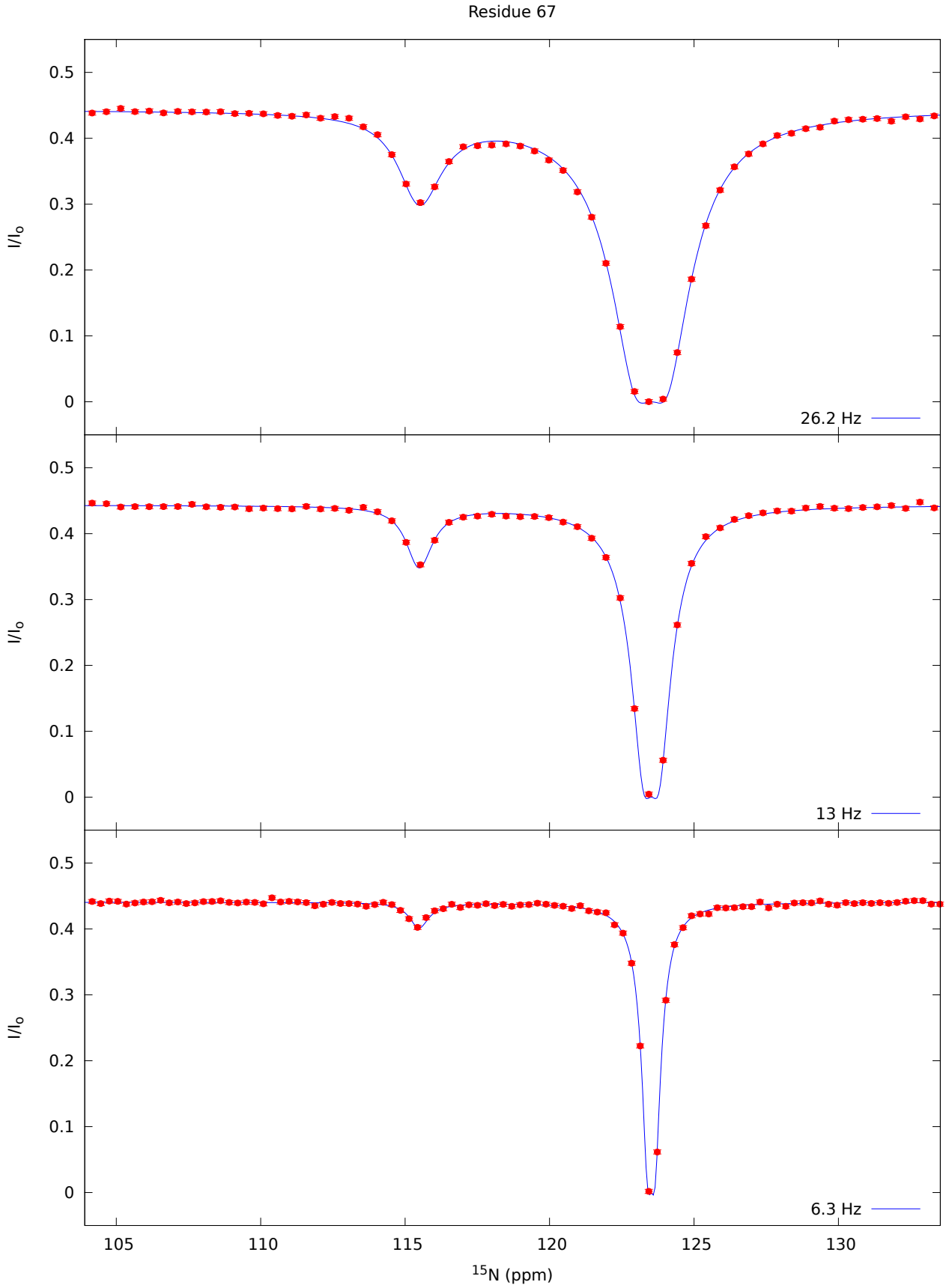
Residue 67
I/I$_o$
0.5
0.4
0.3
0.2
0.1
0
26.2 Hz
13 Hz
6.3 Hz
105
110
115
120
125
130
^{15}N (ppm)

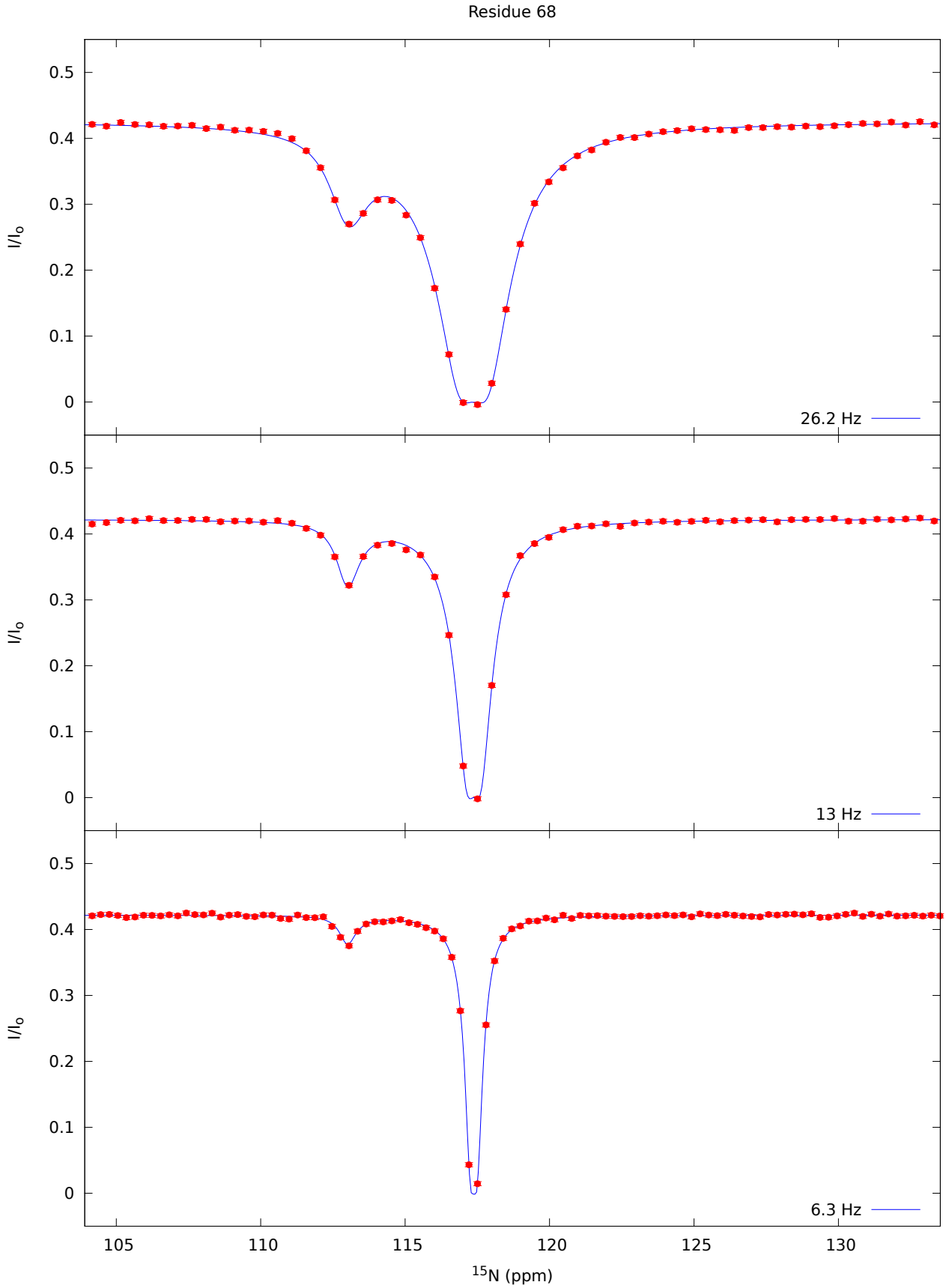
Residue 68
I/I$_o$
0.5
0.4
0.3
0.2
0.1
0
26.2 Hz
13 Hz
6.3 Hz
105
110
115
120
125
130
^{15}N (ppm)

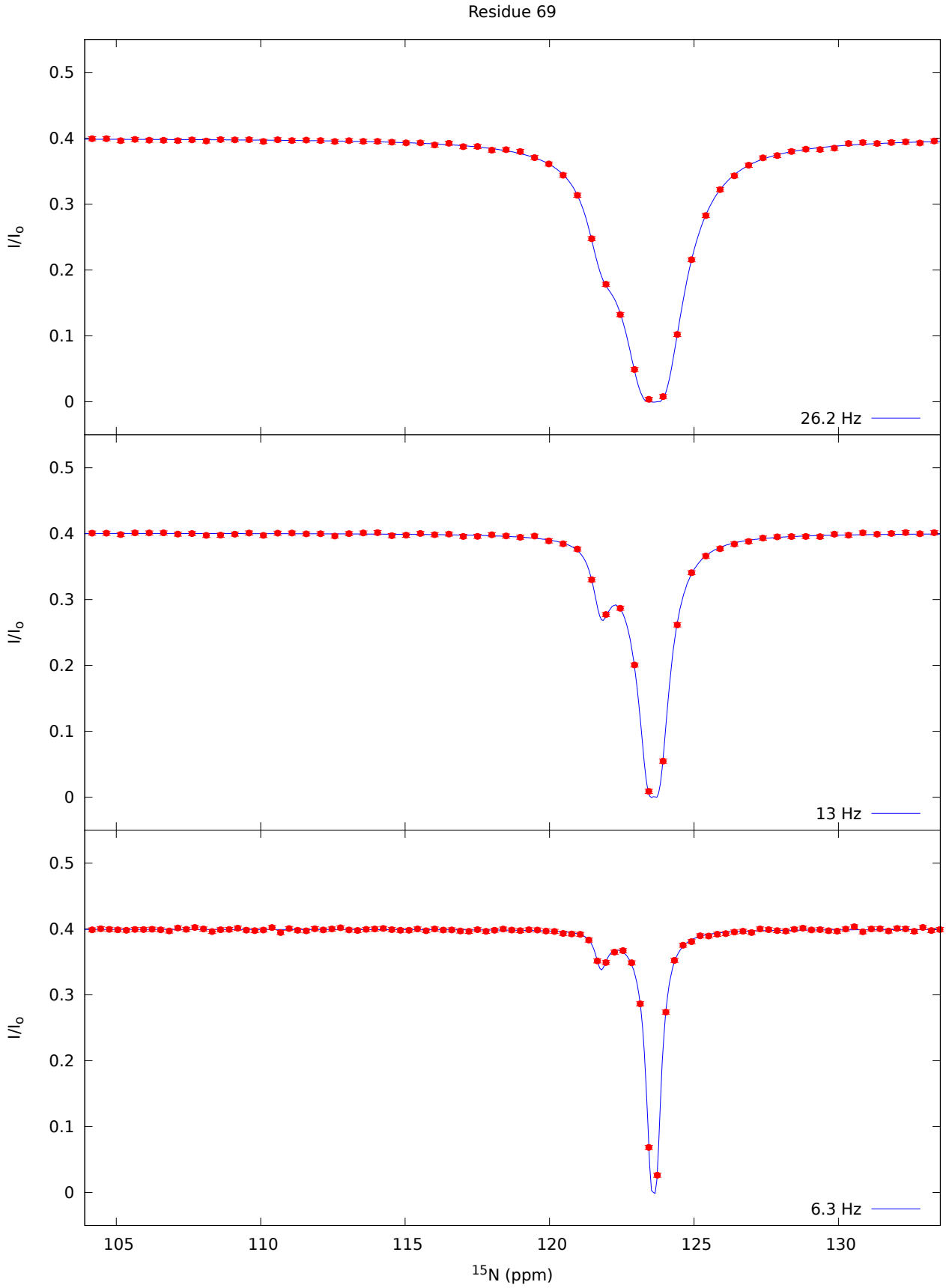
Residue 69
I/I$_o$
0.5
0.4
0.3
0.2
0.1
0
26.2 Hz
13 Hz
6.3 Hz
105
110
115
120
125
130
^{15}N (ppm)